Whitepaper

Breast Care. Because We Care.

Advances in Breast Imaging

siemens-healthineers.com

SIEMENS Healthineers

Image Interpretation Principles of 3D Automated Breast Ultrasound – A Case Based Introduction

Ingolf Karst, MD, PhD, MA[1]; Nadine Gottschalk, MD[2]; Ellen B. Mendelson, MD, FACR[2]; Erin I. Neuschler, MD[3]

[1]Breast Imaging, Northwestern Medicine, Chicago, IL, USA
[2]Department of Radiology, Northwestern University, Feinberg School of Medicine, Chicago, IL, USA
[3]Department of Radiology, University of Illinois at Chicago, College of Medicine, Chicago, IL, USA

Introduction

Background

Dedicated ultrasonic breast scanners were first reported in the 1960s [1, 2]. Over the last 5 decades the development of automated whole breast ultrasound (US) scanners has accelerated by advances in higher US image resolution and increased computational processing power to handle three-dimensional (3D) image-sets in real-time [1–3]. The use of automation to acquire ultrasound images to detect breast cancer is similar to the renaissance of tomography in digital breast tomosynthesis (DBT) in that they both combine a long established imaging technique, ultrasound or tomography, with a newer ability to digitally store and process 3D imaging sets. The use of volumetric images of the breast allows for representation of the entire breast volume as a scrollable stack of images on a workstation monitor. The achieved higher 3D resolution of the breast tissue can result in higher displayed spatial 3D resolution. In comparison, handheld (HH) US and full field digital mammography (FFDM) store images in rather static two-dimensional (2D) projections. When HH US is used, radial and antiradial or transverse and longitudinal planes are frequently used as orthogonal projections to record significant imaging findings in the picture archiving and communication system (PACS). To capture the images in FFDM technique, the mediolateral oblique (MLO) and craniocaudal (CC) views are the most commonly used projections for interpretation. For both mammographic modalities, FFDM and DBT, the use of X-rays is required to radiograph the breast tissue. Unlike with X-ray imaging, no ionizing radiation is necessary to create the images with US high frequency sound waves and with magnetic resonance imaging (MRI). Meanwhile MRI is still in need of contrast medium (CM). In this regard automated ultrasound (AUS) is in today's standard the only modality able to depict the whole breast in a tomographic representation without the use of ionizing radiation or need of contrast medium (Table 1). The clinical benefit of using higher 3D spatial resolution in AUS and DBT is that it may enable better differentiation of benign and malignant findings compared to a static 2D image interpretation. The transition to a volumetric breast examination reading may minimize the masking effect of overlying tissue in DM and the operator dependence in US [4–6]. A more widespread use of volumetric breast ultrasound modality systems however requires evaluation of the advantages and challenges when introduced into the clinical setting to unfold its full

	2D DM	Tomo	HH US	AUS	Breast MRI
Whole breast depicted	**Yes**	**Yes**	No	**Yes**	**Yes**
Tomographic (thin slices)	No	**Yes**	**Yes**	**Yes**	**Yes**
No ionizing radiation (IR) or IV CM	Has IR	Has IR	**Yes**	**Yes**	Has CM
Score	+1	+2	+2	**+3**	+2

Table 1: Breast imaging modalities in clinical use today categorized by the ability to depict the whole breast, to be tomographic in image representation, and the need to use ionizing radiation (IR) or intravenous (IV) contrast medium (CM). Over the last two decades digital breast tomosynthesis (DBT) and automated breast ultrasound (AUS) have become more widespread in clinical use. In addition to Breast MRI, DBT and AUS enable depiction of the whole breast in a tomographic representation. Whereas DBT involves the use of ionizing radiation to produce the images, MRI is currently still in need of IV contrast medium application to provide diagnostic kinetic curve type assessment for classification of breast lesions. AUS however has an advantage since it is tomographic and depicts the whole breast without the need of ionizing radiation or IV contrast medium.

potential. To support the transition from using 2D oriented modalities to a successful clinical integration of 3D modalities, this publication presents material that is based on decade long experience in AUS technology and in production of educational programs benefitting physicians in AUS interpretation. The aim of this article is help transition 3D AUS to a broader audience and to increase specificity and positive predictive values by decreasing false positive interpretation results.

AUS image acquisition and positioning

To acquire the images a wide field of view ultrasound probe with a width of 15.4 cm travels from inferior to superior over the breast tissue to capture the images in a transverse direction. The ultrasound probe is covered by a housing. At the bottom of the housing a one-time use mesh is attached to protect the scanner. The images presented in this article are obtained with an AUS system that scans the patient in a supine position (ACUSON S2000 Automated Breast Volume Scanner; Siemens Healthineers, Mountain View, CA, USA). To yield a better quality of scanned images and to lower the frequency of artifacts while scanning, a coupling lotion is used and is spread evenly over the breast before the scanner is positioned on the patient's breast. While the image-slices are scanned one after another, the images are digitized and stored on the AUS machine. One complete scan cycle is finished in about 60 seconds and forms the original set of images that includes a maximum of 320 images per scan. The original set of images is acquired in the transverse direction and builds the basis for later software processing to reconstruct two additional orthogonal planes per scan, the coronal plane (Z) and the sagittal plane (Y) (Fig. 1).

Usually three scans per breast are obtained to cover all of the breast tissue in the anterior-posterior (AP), lateral (LAT), and medial (MED) position of the transducer. The image-sets resulting from the AP, LAT, and MED positioned scan are identified as views in this article and differentiated from the three orthogonal planes per scan, the transverse, coronal, and sagittal planes.

Reconstruction of additional planes

After acquisition of usually six scans per examination, three per breast, the images are sent to the PACS. When the studies are received by the PACS, the reading software on the physician's workstation allows for interpretation of the AUS examinations. To display the volumetric image-set for interpretation, the acquired transverse plane is reconstructed in two additional orthogonal planes, the coronal and sagittal planes. The coronal plane (Z) as a reconstructed plane depicts the entire breast of a supine positioned patient. On the coronal plane the breast tissue is presented with the patient similarly positioned as for a potential interventional ultrasound guided procedure or breast surgery (Fig. 2). The reconstruction, with the help of the coronal plane, allows for improved depiction of imaging

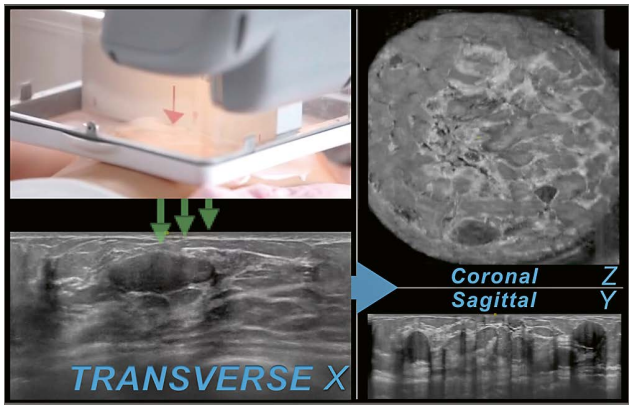

1 **Image acquisition.** The wide field of view ultrasound probe is positioned in anterior-posterior position on the patient's breast. While traveling from the inferior to the superior region of the breast the images are consecutively recorded in the transverse plane (X) (green arrows). An oval parallel circumscribed hypoechoic mass can be seen on the transverse plane in this case of a 29-year-old woman with a history of biopsy-proven fibroadenomas. The same mass is also seen in the inferior region after reconstruction on the coronal plane (Z) as well as the sagittal plane (Y) next to similar appearing lesions in this multiple mass case.

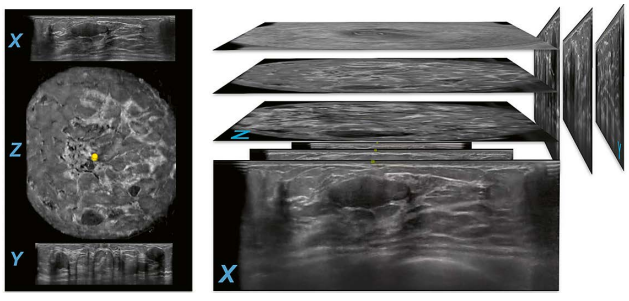

2 **Reconstruction of AUS planes.** Images from the same patient as in Figure 1 are shown. There are at least two circumscribed hypoechoic lesions in the lower region of the breast on the reconstructed coronal plane (Z) of this anterior-posterior (AP) view. The larger more superficial located lesion is in focus on the transverse plane (X). The layer of image-slices in the middle and right portion of the figure demonstrates the transverse plane (X) as the acquired set of images that allows for reconstruction of the two other planes, sagittal (Y) and coronal (Z). The lesion in focus on the transverse plane (X) is also in focus on the reconstructed sagittal plane (Y) and is identifiable as more superficial then the other lesion that is seen in the upper region of the breast on the same sagittal image.

findings such as architectural distortion as well as multiple benign-appearing masses as seen in Figure 2. The darker appearing tissue is fatty and the lighter appearing tissue is fibroglandular. Usually a yellow circle or square denotes the nipple location.

Basic principles in image interpretation

Image interpretation by using AUS-integrated-software
One method to begin the AUS image interpretation is to read both AP-view coronal planes, right and left, side-by-side. Starting at the skin level, scrolling through the reconstructed tissue layers allows for a rapid overview of the anatomic representation. In a bilateral comparison the image findings can be identified by sweeping through the planes towards the chest level (Fig. 3).

During the first cycle of viewing the images, the coronal side-by-side mode enables the bilateral presentation of the anatomy and an overview of findings. Passing the chest level in an upward direction, an area of interest can be further examined in more detail by switching the hanging protocol to the 3 planes in 1 view mode (Fig. 4).

In addition to using the interpretation software to navigate AUS studies, the software includes tools to manipulate the images in real-time. There are a number of integrated tools to support the assessment of AUS exams. Specifically, the Zoom-tool and the Rotate-tool are useful instruments for further lesion characterization, especially on the acquired transverse plane. Figure 5 demonstrates the use of the Zoom-tool to magnify an area of interest.

In other instances, the rotational tool can be helpful to interpret image findings. By simulating tilting and rotating

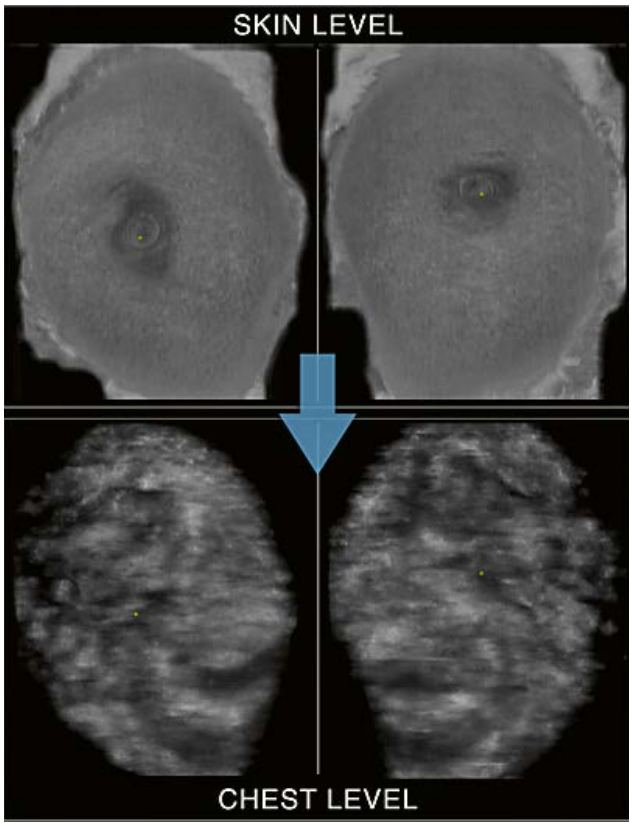

3 **Use of hanging protocols:** Coronal plane side-by-side mode. Starting at the skin level with the right and left coronal planes side-by-side allows for a time saving bilateral interpretation of the anatomy and findings by scrolling through the reconstructed layers towards deeper levels (symbolized by the arrow). At the chest level the pectoralis muscles and rib cage can be identified.

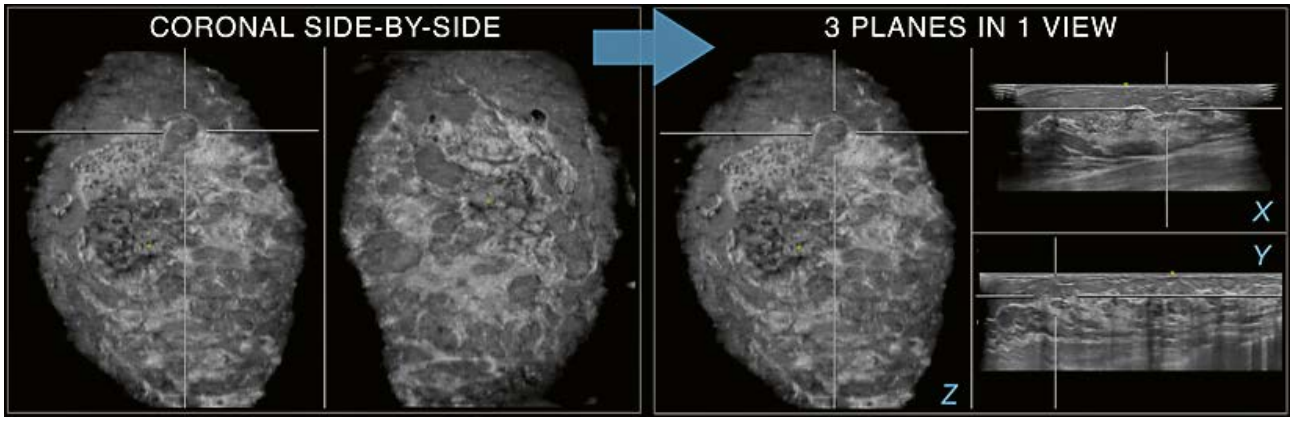

4 **Use of hanging protocols:** Coronal plane side-by-side (coronal side-by-side) and 3 planes in 1 view (3-in-1-view) modes. If an area of interest is focused on the coronal plane, a switch to the 3-in-1-view mode can reveal further details (arrow). In the example shown, the area in crosshairs on the coronal side-by-side is resolved on the 3-in-1-view mode. The targeted area on the coronal plane (Z) may be perceived as an oval circumscribed lesion when only the coronal plane is interpreted. When switched to the 3-in-1-view it becomes apparent that the region in focus represents a fat lobule and summation of cooper ligaments as recognized on the transverse (X) and sagittal (Y) planes, rather than a circumscribed lesion.

of a HH probe in real-time, an area of interest can be further evaluated, such as in cases of conspicuous breast duct findings (Fig. 6).

Benefits of the coronal plane

The coronal plane can provide an overview of all covered breast tissue in one single view. When displayed side-by-side this plane is best for representing the breast anatomy and for rapid recognition of findings. As an example, the radial array of ducts entering the nipple is easily recognized as well as the echogenicity distribution patterns in correlation to the breast composition patterns in mammography. The reconstructed plane facilitates immediate recognition of masses, perceived as holes, and supports judgement of bilateral distribution and multiplicity of findings (Fig. 7). Especially architectural distortion (AD) can easily be identified, for instance recognizable as spiculation in cases of AD involving a malignancy. The conspicuity of AD seen on the coronal plane can be similar to that seen on tomosynthesis.

Image finding resolution

Shadowing is a challenging entity in AUS interpretation. Because of US inherited principles there are a number of reasons that can cause the appearance of shadowing on US images. Some of these reasons are due to US technique and can be artifact, such as ringdown artifact due to a small air bubble between the scanner probe and the skin. Other underlying reasons can be indicators of a true abnormality, such as posterior shadowing of a malignant mass or shadowing due to a surgical scar [5]. Differentiation of particular types of shadowing on AUS can lead to the classification of a finding as an artifact or indicate a true abnormality (Fig. 8). The distinction of findings between artifact and true abnormality can decrease false positive recommendation (FP) such as the recommendation to recall a patient from screening. Distinguishing between true abnormalities not needing further workup, e.g., surgical scar, and suspicious abnormalities, e.g., posterior shadowing associated to a malignancy, can further influence the FP-rate and therefore positive predictive values of physician's recommendation.

Principles to resolve shadowing as a challenging entity

Utilize additional planes to resolve shadowing

Image findings seen on the coronal plane can at times be inconclusive in assessment without utilization of additional planes. In Figure 9 the coronal plane shows an irregular hypoechoic area in the upper region of the breast. If only the coronal plane would be interpreted, the targeted area

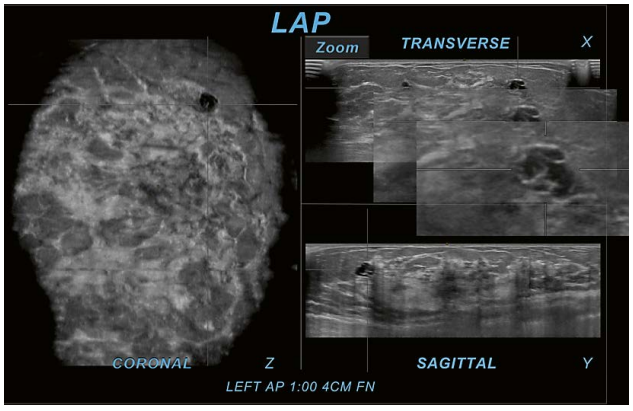

5 **Use of software tools:** Zoom-tool. The Zoom-tool is one of the provided software tools that allows magnification of findings within the interpretation software on the PACS workstation. In this case of a 31-year-old woman with left upper outer quadrant pain, the Zoom-tool is used on the transverse plane (X). The cystic area in crosshairs is located in the upper outer region as identified on the coronal plane (Z). On the sagittal plane (Y) the same area is also identifiable as in the upper region. The use of the Zoom-tool on the acquired plane can increase the confidence to judge the area of interest as a cluster of cysts. The magnification demonstrates only cyst walls without identification of an internal mass or other suspicious findings. This observation allows for a BI-RADS 2 assessment without the necessity for further workup. If this was assessed as BI-RADS 3, then follow-up examinations may also exclude a malignancy. This case was assessed as BI-RADS 2 without a false negative result.

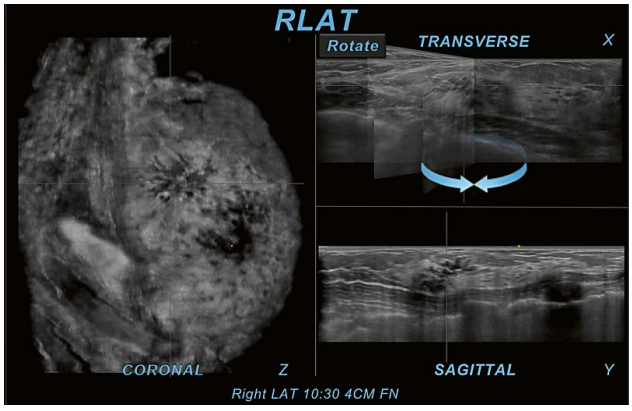

6 **Use of software tools:** Rotate-tool. Here a case of a 43-year-old woman recalled from screening mammography for an asymmetry is shown. There is an area of questioned architectural distortion (AD) and convoluted ducts seen on the coronal plane (Z). The Rotate-tool used on the transverse plane (X) helps the interpreter to follow the tubular structures and identify them as discrete tortuous ducts with associated AD. Due to the associated AD and growth of the area during follow up, the finding was assessed as BI-RADS 4B and recommended for US-guided core biopsy. Histo-pathology yielded flat epithelial atypia (FEA), columnar cell change, apocrine metaplasia, and fibrosis and surgical consultation was recommended.

could represent shadowing associated with an irregular mass. In cases like this, utilization of an additional plane, either the acquired transverse or reconstructed sagittal plane, may help to distinguish between a suspicious and a benign finding. In the case of Figure 9, the use of a second plane clearly reveals the typical pattern of hyperechoic and anechoic horizontal lines originating at the skin with posterior shadowing seen on both additional planes, the transverse as well as the sagittal planes. By identifying this pattern as ringdown, the finding is classified and resolved as an artifact that is caused by interrupted contact between the transducer and the skin because of trapped air while scanning. This artifact can be minimized by an optimal scanning technique and careful application of lotion during the scanning process [5, 9].

Utilize a second view to resolve shadowing

In Figure 10, there is shadowing seen on all three planes on the right AP view (RAP). The shadowing seen in the peripheral region of the RAP view coronal plane is also identified on the RAP transverse and sagittal planes. An underlying suspicious finding cannot be excluded by solely using additional planes as shown in the prior example of ringdown artifact. In cases like this, utilization of a second view can support differentiation of an artifact from a true abnormality and potentially avoid false positive recalls.

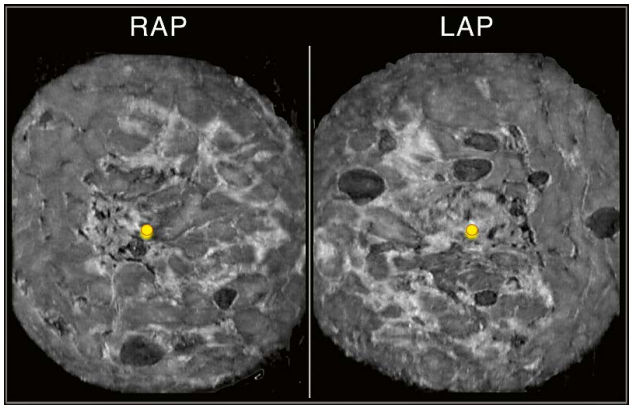

7 Coronal plane. Shown is the right (R) and left (L) anterior-posterior (AP) coronal plane of the same patient as in figure 1 and 2. The bilateral distribution of the multiple masses is easy to appreciate on both coronal planes side-by-side. The use of the reconstructed plane allows for characterization of the presented findings as multiple bilateral similar-appearing circumscribed masses. A BI-RADS 2 category assessment may be appropriate according to published studies supported by ACRIN 6666 data with no malignancies found with at least 2 years of follow-up [7]. "Multiple bilateral masses" is defined here as at least 3 masses in total and at least one per breast [8].

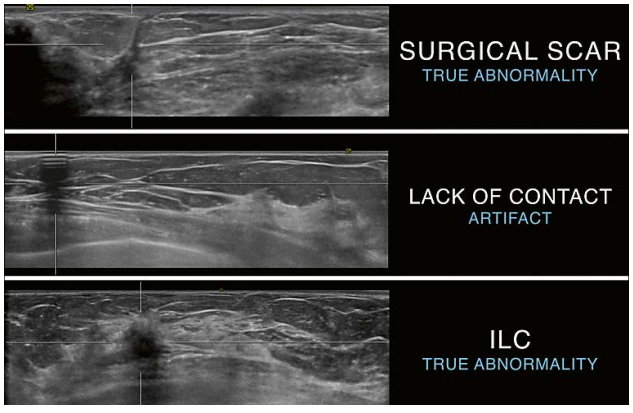

8 Differentiation of shadowing on AUS as indicator for a true abnormality or an artifactual finding. Top: linear shadowing originating at the skin and leading towards the chest level. The appearance is classic for a surgical scar and represents the surgical pathway leading to an excision site. The shadowing is caused by a true abnormality. Middle: shadowing with the typical appearance of alternating hyperechoic and anechoic horizontal lines originating at the skin with posterior shadowing. This pattern confirms ringdown as the cause of shadowing and confirms the presence of an artifact. Bottom: posterior shadowing due to a malignant mass. Due to attenuation of the ultrasound beam passing through a malignant mass, shadowing can be seen posterior to the mass as in this example of an invasive lobular carcinoma (ILC).

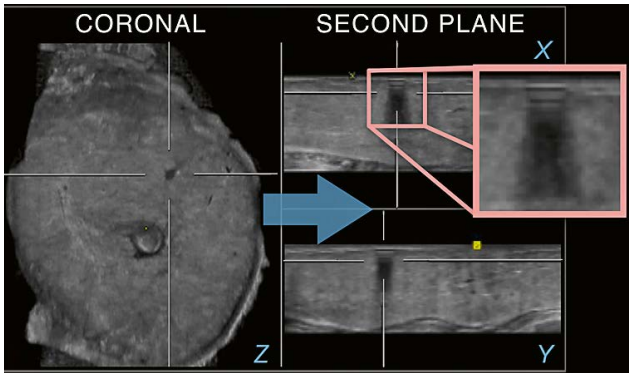

9 Utilization of an additional plane. There is an irregular appearing hypoechoic area in the upper region of the breast seen on the coronal plane (Z). When an additional plane is used (arrow), the finding is clearly resolved as an artifact due to the identification of ringdown on the transverse (X) as well as the sagittal (Y) planes. The typical pattern of ringdown is recognized on the magnification overlaying the transverse plane (square).

Figure 11 illustrates another case utilizing a second view. The peripheral shadowing on the RAP view is again recognized on all three planes. Exclusion of a suspicious finding is again difficult when only this view is interpreted. However, when switched to the second view, the image finding in the same location becomes clearly identifiable as a benign finding. The rim eggshell calcification with posterior shadowing is diagnostic for fat necrosis. Here, the second view helps to classify a true abnormality as a benign finding.

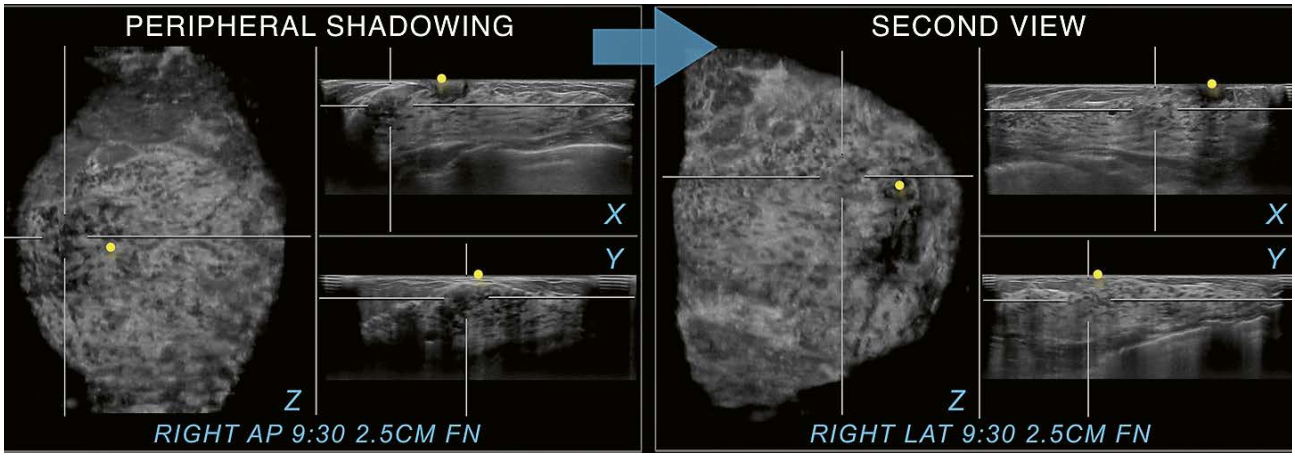

10 Utilization of a second view. Peripheral shadowing is seen on the right AP view coronal plane at the 9:30 position 2.5 cm from the nipple (FN) in this case of a 36-year-old woman with dense breast tissue. The shadowing is also present on both other RAP planes, the RAP transverse and sagittal planes. When the right lateral (LAT) view is selected as a second view to display (arrow), only normal fibroglandular tissue is found in the same position as on the anterior-posterior scan. The second view resolves the peripheral shadowing seen on RAP as artifactual rather than as shadowing caused by an underlying suspicious lesion. The peripheral shadowing now seen at 6 o'clock on the right LAT view coronal plane was resolved in the same way as just demonstrated with the 9:30 o'clock RAP view coronal plane shadowing. Yellow circles mark the nipple region.

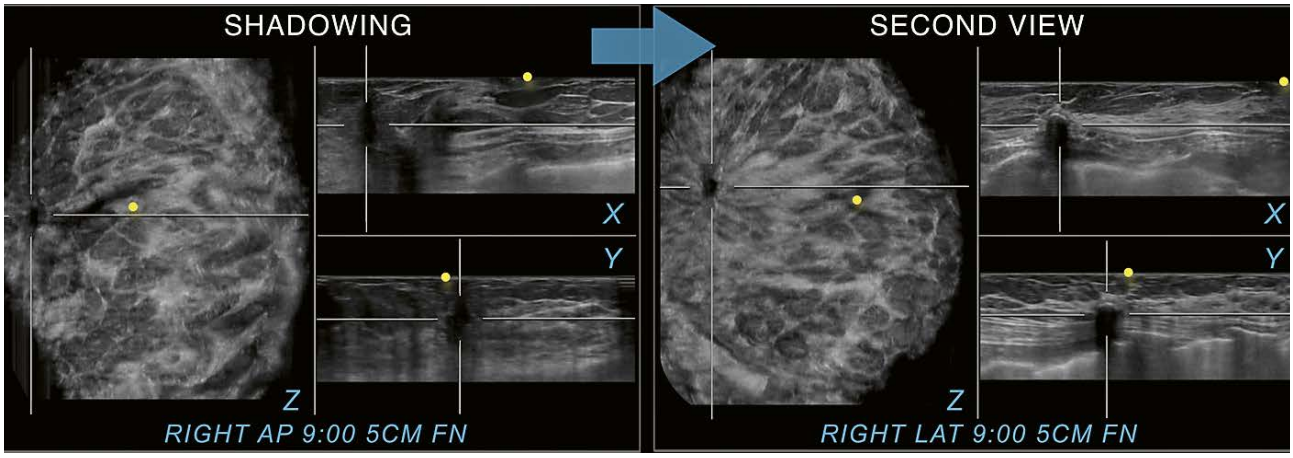

11 56-year-old woman with a history of a lumpectomy on the right. Excisional biopsy ten years ago yielded invasive mammary carcinoma and ductal carcinoma in situ grade 1. The patient returns for diagnostic follow up with shown images. Shadowing next to a surgical scar is seen on all three planes on this RAP view and a recurrence is difficult to exclude. Switching to the second view however allows for identification of the same finding in the same location at 9:00 o'clock and 5 cm FN as fat necrosis. Therefore, the case can appropriately be assessed as BI-RADS 2 and the patient can return to screening. Yellow circles mark the nipple region.

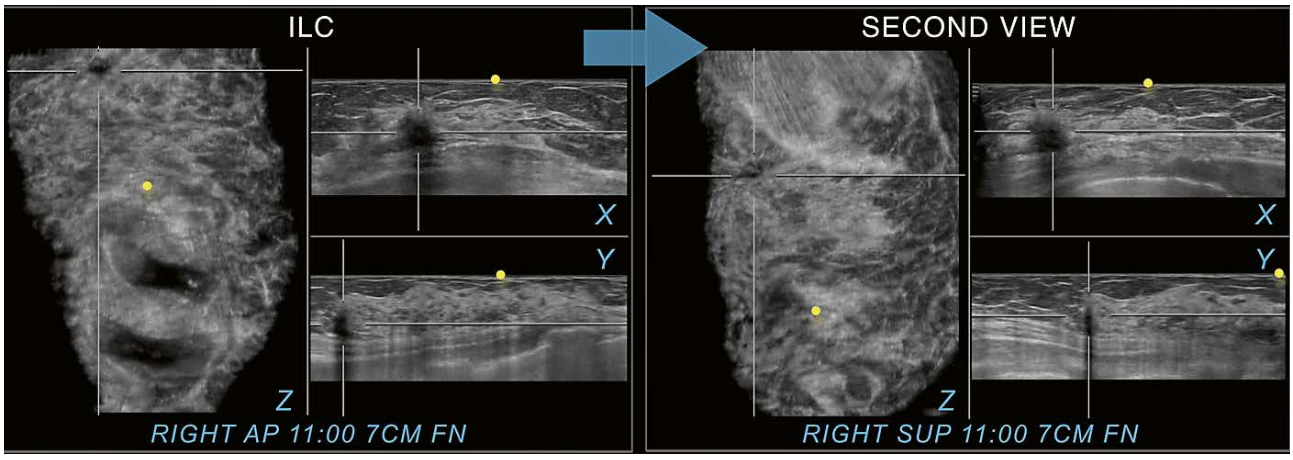

12 Invasive lobular carcinoma (ILC) for comparison. The shadowing caused by a malignant mass is seen in all three planes on the right AP view at 11:00 o'clock 7 cm FN. The right superior view (SUP) as a second view (arrow) supports identification of the same image findings in the same location as seen on the AP view and therefore confirms the finding as associated to a true abnormality. The example illustrates the difference in appearance between shadowing associated with a malignancy and shadowing caused by dense breast tissue in the periphery of a scan, that can be resolved on the second view as shown in figure 10. Yellow circles mark the nipple region.

In comparison, Figure 12 shows shadowing originating from a malignant mass. The shadowing seen posterior to the mass is due to attenuation of the ultrasound beam. The second view confirms the presence of an irregular hypoechoic mass with posterior shadowing and associated AD. As seen in the examples of Figures 10 to 12, utilization of a second view can help to distinguish a true lesion from an artifactual finding. Accurate classification of shadowing as artifactual and not caused by a suspicious finding may lead to a lower FP-rate and thus increase the positive predictive value of recommendations.

Conclusion

Over the last decade automated breast ultrasound (AUS) and digital breast tomosynthesis (DBT) were added to complement three-dimensional modalities available to breast imagers. With an increase in three-dimensional (3D) spatial resolution at AUS and DBT, breast cancer detection may also increase. Nonetheless, adoption of these 3D modalities into daily practice includes reading of additional volumetric imaging information and a potential need to resolve artifacts. In an effort to reduce preventable false-positive recommendations and to resolve findings, utilization of a methodical approach can help differentiate benign from malignant findings on AUS. Identifying the factors which influence the false positive rate, and therefore positive predictive values, may lead to higher accuracy in automated breast ultrasound image interpretation during its more widespread integration into the breast imaging practice.

Contact

Ingolf Karst, MD, PhD, MA
Breast Imaging
Northwestern Medicine
250 E Superior St
Suite 4-2304
Chicago, IL 60611
USA
ikarst@nm.org

References

1 Dempsey PJ. The history of breast ultrasound. J Ultrasound Med 2004; 23:887-894.
2 Maturo VG, Zusmer NR, Gilson AJ, et al. Ultrasound of the whole breast utilizing a dedicated automated breast scanner. Radiology 1980; 137:457-463.
3 Wojcinski S, Farrokh A, Hille U, et al. The Automated Breast Volume Scanner (ABVS): initial experiences in lesion detection compared with conventional handheld B-mode ultrasound: a pilot study of 50 cases. Int J Womens Health 2011; 3:337-346.
4 Hooley RJ, Durand MA, Philpotts LE. Advances in Digital Breast Tomosynthesis. AJR Am J Roentgenol 2017; 208:256-266.
5 Karst I, Henley C, Gottschalk N, Floyd S, Mendelson EB. Three-dimensional Automated Breast US: Facts and Artifacts. Radiographics 2019:180104.
6 Vourtsis A, Kachulis A. The performance of 3D ABUS versus HHUS in the visualisation and BI-RADS characterisation of breast lesions in a large cohort of 1,886 women. Eur Radiol 2018; 28:592-601.
7 Berg WA, Zhang Z, Cormack JB, Mendelson EB. Multiple bilateral circumscribed masses at screening breast US: consider annual follow-up. Radiology 2013; 268:673-683.
8 Leung JW, Sickles EA. Multiple bilateral masses detected on screening mammography: assessment of need for recall imaging. AJR Am J Roentgenol 2000; 175:23-29.
9 van Zelst JCM, Mann RM. Automated Three-dimensional Breast US for Screening: Technique, Artifacts, and Lesion Characterization. Radiographics 2018:170162.

Digital Breast Tomosynthesis in Screening – Approaches to Reduce Reading Time

Ioannis Sechopoulos, PhD

Department of Radiology and Nuclear Medicine, Radboud University Medical Center, Nijmegen, The Netherlands
and Dutch Expert Center for Screening (LRCB), Nijmegen, The Netherlands

Abstract

The development of digital breast tomosynthesis (DBT) for the detection of breast cancer has resulted in many trials showing that an improvement in detection is possible with DBT. However, these trials have also shown that reading DBT images is considerably slower than reading standard digital mammography (DM) cases. Not surprisingly, it takes longer to read a stack of 50 image slices than one standard mammogram. This increase in reading time for DBT interpretation limits its introduction in large screening programs, such as the regional or national screening programs commonly found in Europe. Therefore, for the better part of this decade, multiple efforts and research have taken place to demonstrate the feasibility of different time-saving strategies when reading DBT exams. As a result, it now seems more feasible than ever that the reading time in DBT could be reduced to match or even be lower than that of DM. For these strategies to be introduced in every-day use, however, some additional studies are needed. Here, we review the strategies proposed up to now to reduce the time required for interpretation of DBT cases in breast cancer screening, and discuss the current limitations in knowledge regarding some of these interpretations.

Introduction

Since digital mammography (DM) is a two-dimensional imaging modality, mammograms of the three-dimensional breast suffer from the phenomenon of tissue superposition. That is, tissues that are separated only vertically in the breast during compression are projected to the same location in the mammogram. This can result in either normal tissues resembling a malignant finding, lowering specificity, or normal tissue masking a real finding, lowering sensitivity. Of course, the higher the proportion of the breast that is composed of dense fibroglandular tissue, the higher the risk of superposition. To ameliorate this effect, currently a mammographic examination, especially for screening for breast cancer, involves the acquisition of two views; the cranio-caudal (CC) and the medio-lateral oblique (MLO) views. However, this is not a perfect solution, since the loss of performance due to this effect, especially in dense breasts, persists.

Digital breast tomosynthesis (DBT) was introduced mostly to reduce this problem of tissue superposition. DBT involves the acquisition of multiple low-dose mammography-like projections from various angles over a limited angular range around the compressed breast (Fig. 1). These projections are then used to reconstruct a pseudo-3D volume depicting the breast tissue distribution [1–3]. This pseudo-3D volume is enough to reduce the impact of tissue superposition despite limited vertical spatial resolution, and results in improved clinical performance compared to DM [4–10].
However, a single DBT image typically consists of a stack of ~50 slices for a breast with a typical thickness under compression of about 50 mm. This increases the amount of information generated by DBT to be reviewed by the interpreting radiologist, which results in a reading time

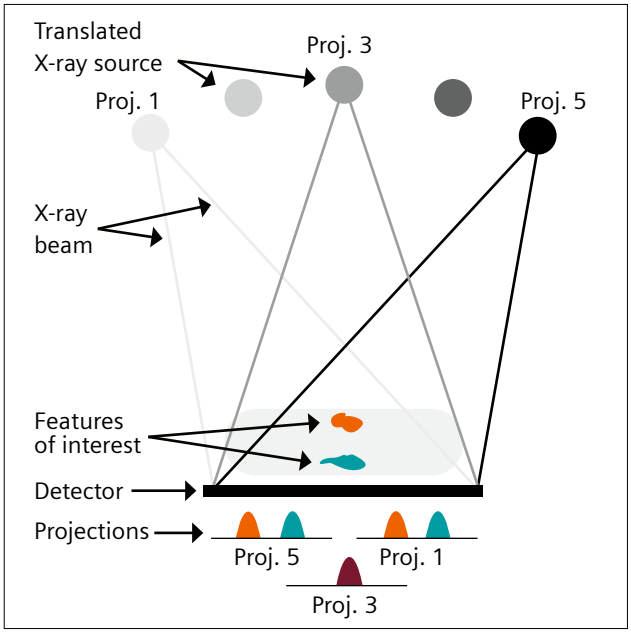

1 Schematic of a digital breast tomosynthesis acquisition, showing a geometry equal to that used in mammography, but with the X-ray source rotating around the compressed breast, acquiring a projection image at each position. The changing X-ray source position results in different projection images, with the features in the breast changing location in the images depending on their vertical location.

that has been repeatedly reported to be double that of DM [11]. This increase in the demand of radiologist resources is one of the most important challenges needing to be overcome before DBT could be introduced in large population screening programs as a replacement of DM. However, several alternative acquisition and reading strategies may be useful in optimizing the interpretation of DBT-based screening. This would allow for the potential of DBT, and its promise of improved outcomes, to finally be introduced in high-volume screening programs without a substantial increase in the expenditure of healthcare resources. The strategies and alternatives that have been proposed or are being investigated can be divided into two categories: alternative strategies to reduce the number of images that need to be interpreted, and strategies to read DBT faster.

Reduction of images to be read

As mentioned, currently a screening DM examination consists of the acquisition of two views per breast. The main reason for this is the attempt to ameliorate the effects of tissue superposition. Since this effect is, to a great extent, solved by DBT, then perhaps it is feasible to not acquire two views of each breast, and therefore, only acquire MLO DBT views during screening. If this were the case, the MLO view would be the chosen one due to it being the view with the largest tissue coverage.

The Malmö Breast Tomosynthesis Screening Trial (MBTST) involved the comparison of the screening performance of such a DBT acquisition strategy (MLO view-only), to that of two-view DM [5, 6]. In this prospective screening trial involving almost 15,000 cases, the use of single-view DBT resulted in an increase in the cancer detection rate of 34% over that obtained in the two-view DM arm; from 6.5 to 8.7 cancers per 1,000 women screened [6]. This strategy also resulted in an important increase in the recall rate of 44% (from 2.5% to 3.6%). However, the baseline recall rate was very low to begin with, and the DBT review did not include the use of prior images, an effective tool that is known to reduce recall rate substantially [12]. In a retrospective observer study, Rodriguez Ruiz et al. compared the detection performance resulting from interpreting single-view DBT to that of single-view DBT + single-view DM, two-view DBT + two-view DM, and two-view DM only [13]. Although the retrospective, enriched case set nature of this study of course involved fewer cases than that in the MBTST, this trial allowed for the evaluation of multiple acquisition strategies, with all cases of all strategies interpreted by all participating radiologists. The authors did not detect any difference in performance among the four acquisition strategies. Therefore, it seems feasible that single-view DBT could be used for screening for breast cancer. However, both of these studies used the same wide-angle DBT system. Therefore, the generalizability of these results to DBT imaging performed with narrower-angle systems remains to be evaluated.

In European population screening programs, the most common standard is that all cases are double read by two different breast radiologists. Two other prospective trials, as part of their investigation into screening DBT, tested the hypothesis that the reduction in superposition effects with DBT results in images being easier to interpret, and therefore double reading not yielding as large an improvement as with DM. In the STORM trial, Houssami et al. determined that single-reading of DM+DBT still resulted in an increase of over 40% in the cancer detection rate and a 26% reduction in recall rate, compared to double-reading DM alone [14]. An important improvement in performance was also detected by Romero Martin et al. as part of the prospective DBT trial in Cordoba, Spain [15]. In that study, the increase in the cancer detection rate with single-reading of DBT with a synthetic mammogram (a mammogram-like image generated from the DBT data) was over 20% compared to that with DM alone, while recall rate was reduced by over 40%.

With the introduction of AI-based automated systems that seem to be approaching, if not already have matched, human performance in interpreting breast images, both DM and DBT (16,17), it is now feasible to think that an AI system could be used to interpret all images, and that only the ones picked out as being more suspicious would need to be reviewed by a breast radiologist. This concept of triaging of normal cases has been investigated by a number of different research groups, all, for now, on DM images, having found that an important reduction in caseload can be achieved (ranging from 20% to 90%), with no loss in overall performance [18–20]. Given the similarity in the results of studies that have compared the stand-alone performance of such AI systems for DM and DBT, it could be expected that the same performance when using these systems for triaging of normal cases would be achievable. However, before such triaging could be introduced in the screening realm, its impact on large-scale screening programs would have to be evaluated prospectively with real screening prevalence. This is especially important since it could be expected that the radiologists' behavior will be affected when facing a case set that has been through triaging by an AI system. Therefore, prospective clinical trials that gauge this impact are necessary.

Faster reading of images

The three strategies discussed above aim to reduce the number of images that are acquired or need interpretation by a breast radiologist. Once this number has been optimized, it would be beneficial to also minimize the time spent in interpreting each of these images. For this, two strategies have been proposed, the use of slabbing, and the synthetic image-driven interpretation of the case.

To understand the motivation for presenting the reconstructed DBT volume as a few slabs instead of many thin slices, it should be noted that the spatial resolution in the vertical direction in DBT is very poor. Given the narrow angles subtended during a complete DBT acquisition (the tube movement of the widest angle DBT system covers an angular range of 50°), the DBT "volume" is actually composed of highly non-isotropic voxels. The signals in the vertical direction included in one voxel can be considerably farther away than the 1 mm often mis-quoted as the slice thickness. In DBT, the slices are reconstructed 1 mm apart from each other, but this does not mean that they are 1 mm thick. In fact, information from 5 mm or more away from the center of the slice may be included in a DBT slice [21]. Therefore, it could be logical that instead of dividing up a typical 50 mm thick breast into fifty 1 mm slices, such a breast could be depicted with considerably fewer, but thicker, slabs. Interpretation of these thicker slabs could be expected to take less time than interpretation of many more thinner slices. However, it should be ensured that all data required to produce a tomosynthesis volume is available in post-processing, meaning the reader can still choose to see the 1mm slices after scrolling through the 8 mm slabs. In a pair of studies evaluating this hypothesis, it was found that using 2 mm thick slabs resulted in a reduction of 20% in the reading time, while still rendering all lesions visible [22, 23]. In another study, Agasthya et al. compared the reading time and performance when radiologists interpreted 8 mm slabs that overlapped by 3 mm to that of interpreting the regular slices (Fig. 2) [24]. The use of the slabbing technique resulted in equal detection performance with a 30% reduction in the reading time.

Another reading strategy that could substantially reduce the reading time per image is using the synthetic mammogram as the primary image for detection, instead of the reconstructed DBT stack. Under such a scenario, the DBT stack would not be reviewed by the radiologist to detect suspicious findings. Rather, the interpreting radiologist would review the synthetic mammogram, and, if any suspicious area is detected, he/she would, if needed, review that area in the DBT stack to determine if that is, indeed, a finding that needs to be recalled, or an innocuous consequence of tissue superposition or other effect on the synthetic mammogram. An early study evaluating the feasibility of such an approach was performed by Murphy et al., finding that although 13% of the cancers included in the study would have been downgraded in suspicion, they still warranted recall, and therefore they would not have been missed [25]. It should be pointed out, however, that this is, as of now, not yet the intended use of the synthetic mammogram, and there are still probably many improvements that are needed in the generation of these images before they can be reliably used as the primary source for detection of actionable findings. However, with the advent of improved algorithms for constructing these synthetic images, probably in the future with AI having a role in this aspect, it can be expected that this could be a viable strategy in the future, especially for the interpretation of "easier" cases.

Conclusion

It can be expected that all or a combination of these time-saving strategies, be they to acquire fewer images, have fewer images be interpreted by breast radiologists thanks to their interpretation by stand-alone AI systems, and/or by reading each image faster, could result in DBT-based screening requiring the same, or fewer, resources as current DM-based screening, while resulting in improved lesion detection performance. For some of these strategies there is still a lot of evidence that needs to be gathered, or algorithms that need improvement, although some of them seem to be closer to implementation. In either case, demands on breast radiologists to reduce the time to make DBT screening in large population programs a reality seems feasible, soon.

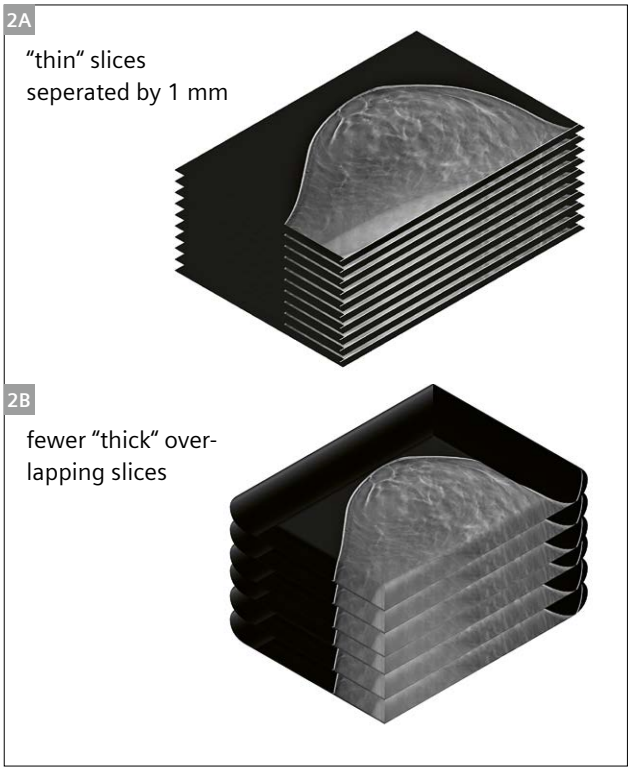

2 Comparison between two stacks of images: (**2A**) thin slices separated by 1 mm; (**2B**) thick partially overlapping slabs. For example, combining 8 slices together with an overlap of three slices results in a five-fold reduction in the number of images in a stack.

References

1 Niklason LT, Christian BT, Niklason LE, Kopans DB, Castleberry DE, Opsahl-Ong BH, et al. Digital tomosynthesis in breast imaging. Radiology. 1997 Nov;205(2):399–406.
2 Sechopoulos I. A review of breast tomosynthesis. Part I. The image acquisition process. Med Phys. 2013 Jan;40(1).
3 Sechopoulos I. A review of breast tomosynthesis. Part II. Image reconstruction, processing and analysis, and advanced applications. Med Phys. 2013 Jan;40(1).
4 Friedewald SM, Rafferty EA, Rose SL, Durand MA, Plecha DM, Greenberg JS, et al. Breast Cancer Screening Using Tomosynthesis in Combination With Digital Mammography. JAMA. 2014 Jun 25;311(24):2499.
5 Lång K, Andersson I, Rosso A, Tingberg A, Timberg P, Zackrisson S. Performance of one-view breast tomosynthesis as a stand-alone breast cancer screening modality: results from the Malmö Breast Tomosynthesis Screening Trial, a population-based study. Eur Radiol. 2016;26(1):184–90.
6 Zackrisson S, Lång K, Rosso A, Johnson K, Dustler M, Förnvik D, et al. One-view breast tomosynthesis versus two-view mammography in the Malmö Breast Tomosynthesis Screening Trial (MBTST): a prospective, population-based, diagnostic accuracy study. The Lancet Oncology. 2018 Nov;19(11):1493–503.
7 Gilbert F, Tucker L, Gillan M, Willsher P, Cooke J, Duncan K, et al. The TOMMY trial: a comparison of TOMosynthesis with digital MammographY in the UK NHS Breast Screening Programme. Health Technol Assess. 2015 Jan 1;19(4).
8 Skaane P, Bandos AI, Niklason LT, Sebuødegård S, Østerås BH, Gullien R, et al. Digital Mammography versus Digital Mammography Plus Tomosynthesis in Breast Cancer Screening: The Oslo Tomosynthesis Screening Trial. Radiology. 2019 Feb 19;182394.
9 Bernardi D, Macaskill P, Pellegrini M, Valentini M, Fantò C, Ostillio L, et al. Breast cancer screening with tomosynthesis (3D mammography) with acquired or synthetic 2D mammography compared with 2D mammography alone (STORM-2): a population-based prospective study. The Lancet Oncology. 2016;17(8):1105–13.
10 Houssami N, Skaane P. Overview of the evidence on digital breast tomosynthesis in breast cancer detection. The Breast. 2013;22(2):101–8.
11 Skaane P, Bandos AI, Gullien R, Eben EB, Ekseth U, Haakenaasen U, et al. Prospective trial comparing full-field digital mammography (FFDM) versus combined FFDM and tomosynthesis in a population-based screening programme using independent double reading with arbitration. Eur Radiol. 2013 Aug;23(8):2061–71.
12 Roelofs AAJ, Karssemeijer N, Wedekind N, Beck C, van Woudenberg S, Snoeren PR, et al. Importance of Comparison of Current and Prior Mammograms in Breast Cancer Screening. Radiology. 2007 Jan 1;242(1):70–7.
13 Rodriguez-Ruiz A, Gubern-Merida A, Imhof-Tas M, Lardenoije S, Wanders A, Andersson I, et al. One-View Digital Breast Tomosynthesis as a Stand-Alone Modality for Breast Cancer Detection: Do We Need More? Eur Radiol. 2018;28(5):1938–48.
14 Houssami N, Macaskill P, Bernardi D, Caumo F, Pellegrini M, Brunelli S, et al. Breast screening using 2D-mammography or integrating digital breast tomosynthesis (3D-mammography) for single-reading or double-reading – Evidence to guide future screening strategies. European Journal of Cancer. 2014 Jul;50(10):1799–807.
15 Romero Martin S, Raya Povedano JL, Cara Garcia M, Santos Romero AL, Pedrosa Garriguet M, Alvarez Benito M. Prospective study aiming to compare 2D mammography and tomosynthesis + synthesized mammography in terms of cancer detection and recall. From double reading of 2D mammography to single reading of tomosynthesis. Eur Radiol. 2018 Jan 2; 28(6):2484-91.y
16 Rodriguez-Ruiz A, Lång K, Gubern-Merida A, Broeders M, Gennaro G, Clauser P, et al. Stand-Alone Artificial Intelligence for Breast Cancer Detection in Mammography: Comparison With 101 Radiologists. J Natl Cancer Inst. 2019 Sep 1;111(9):916–22.
17 Conant EF, Toledano AY, Periaswamy S, Fotin SV, Go J, Boatsman JE, et al. Improving Accuracy and Efficiency with Concurrent Use of Artificial Intelligence for Digital Breast Tomosynthesis. Radiology: Artificial Intelligence. 2019 Jul 1;1(4):e180096.
18 Rodriguez-Ruiz A, Lång K, Gubern-Merida A, Teuwen J, Broeders M, Gennaro G, et al. Can we reduce the workload of mammographic screening by automatic identification of normal exams with artificial intelligence? A feasibility study. Eur Radiol. 2019 Sep 1;29(9):4825–32.
19 Yala A, Schuster T, Miles R, Barzilay R, Lehman C. A Deep Learning Model to Triage Screening Mammograms: A Simulation Study. Radiology. 2019 Aug 6;293(1):38–46.
20 Kyono T, Gilbert FJ, van der Schaar M. Improving Workflow Efficiency for Mammography Using Machine Learning. Journal of the American College of Radiology. 2019 May 30 17(1PA):56-63.21 Rodríguez-Ruiz A, Castillo M, Garayoa J, Chevalier M. Evaluation of the technical performance of three different commercial digital breast tomosynthesis systems in the clinical environment. Physica Medica. 2016 Jun 1;32(6):767–77.
21 Rodríguez-Ruiz A, Castillo M, Garayoa J, Chevalier M. Evaluation of the technical performance of three different commercial digital breast tomosynthesis systems in the clinical environment. Physica Medica. 2016 Jun 1;32(6):767–77.
22 Dustler M, Andersson M, Förnvik D, Timberg P, Tingberg A. A study of the feasibility of using slabbing to reduce tomosynthesis review time. Proc SPIE. 2013;8673:86731L-86731L – 6.
23 Petersson H, Dustler M, Tingberg A, Timberg P. Evaluation of the possibility to use thick slabs of reconstructed outer breast tomosynthesis slice images. Proc of SPIE 2016 ;9787:97871M.
24 Agasthya GA, D'Orsi CJ, Holbrook A, Ho C, Piraner M, Newell M, et al. Reduction in digital breast tomosynthesis interpretation time by slabbing of the reconstructed slices. In: European Congress of Radiology. Vienna, Austria; 2016.
25 Murphy MC, Coffey L, O'Neill AC, Quinn C, Prichard R, McNally S. Can the synthetic C view images be used in isolation for diagnosing breast malignancy without reviewing the entire digital breast tomosynthesis data set? Irish Journal of Medical Science. 2018 9 2018 Nov;19(11):1493-1503.

Contact

Ioannis Sechopoulos, PhD
Associate Professor
Department of Radiology and
Nuclear Medicine Radboud University
Medical Center
P.O. Box 9101, Route 766
6500 HB Nijmegen
The Netherlands, and
Dutch Expert Center for Screening (LRCB)
Nijmegen, The Netherlands
ioannis.sechopoulos@radboudumc.nl

Artificial Intelligence to Help Radiologists in the Early Detection of Breast Cancer with Mammography and Breast Tomosynthesis

Alejandro Rodríguez-Ruiz, PhD and Nico Karssemeijer, PhD

ScreenPoint Medical BV, Nijmegen, The Netherlands

Siemens Healthineers and ScreenPoint Medical are partners committed to developing artificial intelligence based applications for breast imaging. This collaborative arrangement also includes the acquisition of a strategic minority stake in ScreenPoint Medical by Siemens Healthineers.

From CAD to AI systems

Since the 1990s, computer-aided detection (CAD) systems have been developed to automatically detect and mark suspicious breast lesions in mammograms, aiming to prevent overlooking of cancers especially in screening programs. Unfortunately, despite the wide implementation of these systems in clinical practice, no studies to date have found that mammography screening cost-effectiveness improves when radiologists use CAD systems [1]. This could be ascribed to two main limitations of these traditional systems: their low specificity (high false positive rate), and their simplistic radiologist-computer interaction by simply displaying marks [2]. Consequently, such low specificity also precludes the use of traditional CAD as a stand-alone reader for screening mammography.

However, the era of traditional CAD as the only possibility to support radiologists reading mammograms could be coming to an end, due to the rise of a new type of systems based on high-accuracy artificial intelligence (AI) algorithms. The success of novel machine learning algorithms based on deep learning convolutional neural networks is rapidly elevating the field of AI for medical imaging [3]. For mammography, AI systems hold the promise to succeed where traditional CAD failed [4, 5].

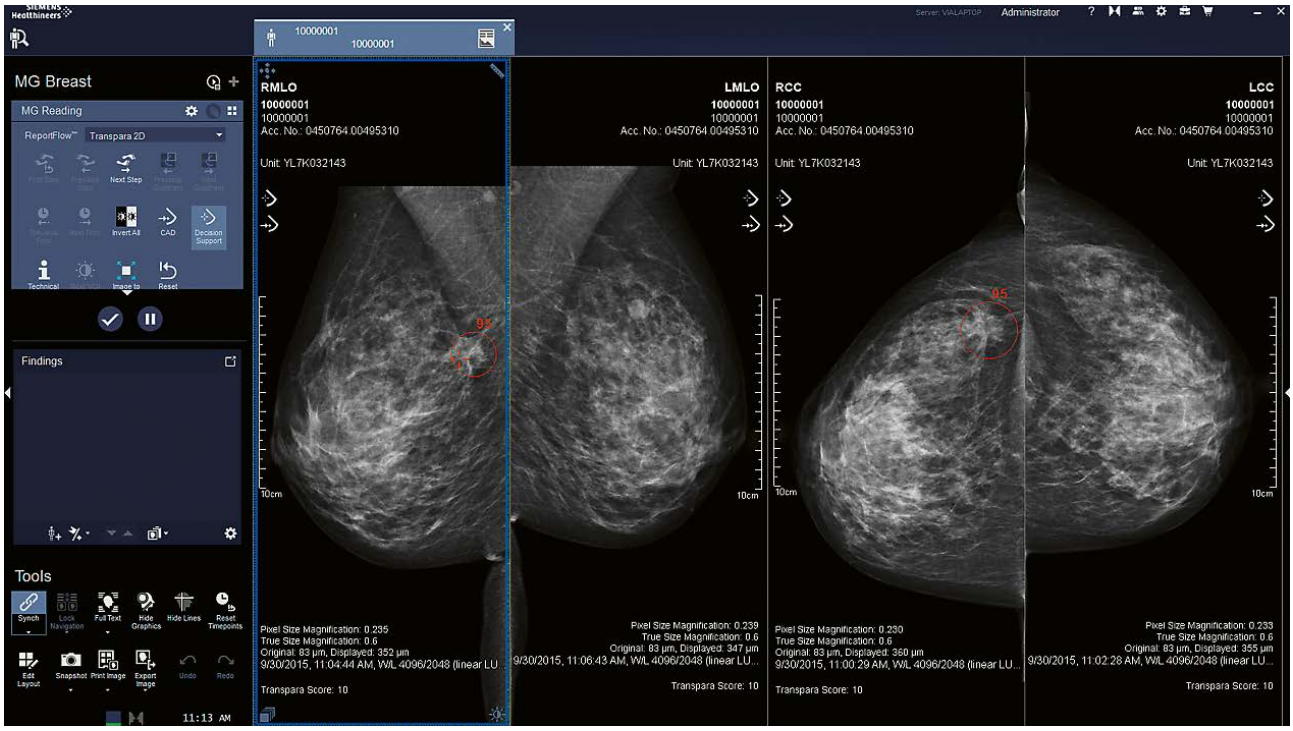

1 Example of the Transpara™ user interface in *syngo*.via (Siemens Healthineers) featuring decision support (circled area in mammogram with likelihood of cancer score, in this case 95, for an area which after biopsy was confirmed as an invasive ductal carcinoma) and the Transpara™ Score (bottom of the image viewport).

In recent years, several deep learning-based algorithms for automated analysis of mammograms have been investigated, some of which have already shown very promising stand-alone detection results in experimental scenarios [6, 7]. The high-performance level of these new AI algorithms can allow the development of systems that can provide radiologists with an enhanced level of support, not simply displaying marks, but that can go deeper into diagnostic decisions such as determining the risk of a lesion representing cancer or confidently determining which screening exams do not contain any suspicious abnormality.

Improving reader accuracy – with focus on lowering the number of mammographically-detected cancers missed at screening – and reducing workload without compromising quality are the aims of most of the latest breast imaging AI systems. In this paper, we summarize the initial clinical evidence conducted with one of the first developed AI systems for mammography and breast tomosynthesis: Transpara™.

What is Transpara™ AI? Features and evidence-based validated performance

Transpara™ (ScreenPoint Medical BV, Nijmegen, The Netherlands) is a deep learning-driven AI system developed after decades of research in breast imaging and automated detection of lesions in mammograms at the Radboud University in Nijmegen. This AI system is FDA cleared for 2D and CE marked for 2D mammography (DM) and breast tomosynthesis (DBT), and can be used in different reading workstations, as shown in one example in Figure 1. This AI system was designed to aid radiologists reading mammograms, by exploiting the latest developments in deep learning algorithms in combination with deep knowledge of mammography imaging physics and radiological patterns of breast cancer.

The AI system automatically detects breast cancer lesions in DM and in DBT exams from most mammography vendors [6, 8]. It has been trained with millions of examples of breast cancer, benign abnormalities, and normal tissue, all validated by biopsy results or follow-up exams. These images originate from a large multi-center and multi-vendor database representing a wide variation of techniques encountered in mammography practices. The results of the computations are presented to the user in two different features:

- **Interactive decision support:** during reading, users can query a mammographic region using a pointer. As a response, Transpara™ provides a region-specific level of suspicion (range 1–100, 100 meaning the highest suspicion for malignancy) as a second opinion. Additionally, suspicious regions-of-interest can be also automatically marked to reduce potential oversight errors with significantly less false positives than traditional CAD systems.
- **Exam-based Transpara™ score:** based on all the individual findings, each exam receives a score ranging from 1 to 10, depicting the increasing risk that the exam contains cancer. The screening mammograms are equally divided across score categories (10% in each), meaning that cancer prevalence is much higher in category 10 than in the rest (see Figure 2). If no potential abnormalities are found, a low score is assigned. The highest scores are assigned to exams with suspicious findings. Exam-scores are possible given the high performance of deep learning algorithms, and where not available with traditional CAD systems.

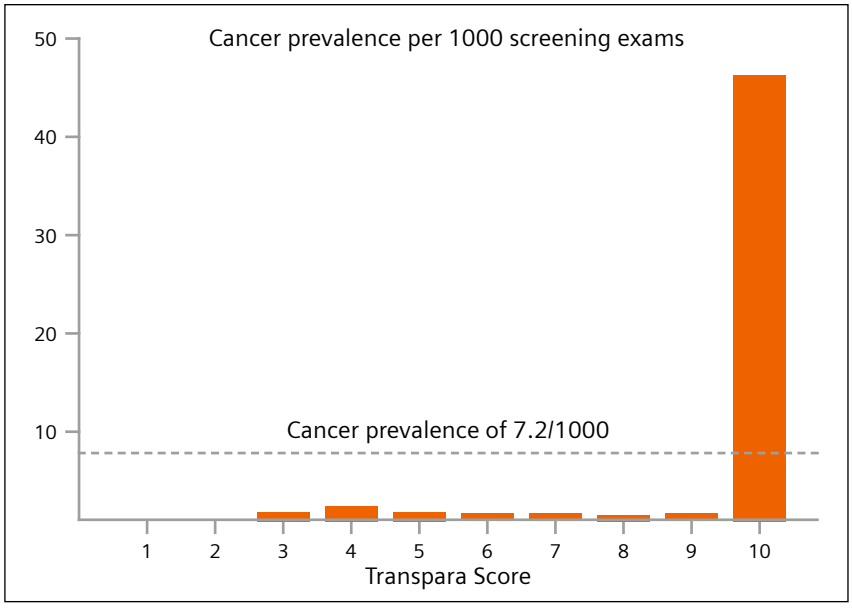

2 Distribution of the Transpara™ Score (version 1.6.0) in a consecutive screening population of 12,245 screening 2D mammograms acquired with a Siemens Healthineers MAMMOMAT Revelation with 88 screen-detected cancers (cancer detection rate = 7.2/1000). In a screening setting, the AI system places 10% of the screening exams on each category, but the cancer prevalence is significantly higher in the highest category 10.

According to two recent comprehensive studies using multi-center independent data [9, 10], the stand-alone breast cancer detection of the AI system (versions 1.3.0 and 1.4.0) has been demonstrated to be as good as that of radiologists.

This independent evaluation data originated from eleven sites across the USA and Europe, adding up to around 3,000 exams with over 700 biopsy-proven mammograms with cancer. The mammograms were acquired with devices of four different mammography vendors (Siemens Healthineers, Hologic, Philips, General Electric). Each exam was read by several radiologists, where in a total of 115 radiologists were included in this study. As a result, the AI system stand-alone interpretation of mammograms was compared to more than 30,000 radiologists' interpretations.

The breast cancer detection performance of Transpara™ in DM was compared to the performance of radiologists in terms of area under the receiver operating characteristic curve (AUC) using a predefined non-inferiority margin of 0.05. In the first study, the AUC of AI was non-inferior to the average AUC of 101 radiologists (0.841 vs. 0.814, AI had 0.027 higher AUC, 95% CI of AUC difference = [-0.003,0.055]). Similarly, In the second study, the AUC of AI was non-inferior to the average AUC of 14 radiologists (0.887 vs. 0.866, AI had 0.021 higher AUC, 95% CI of AUC difference = [-0.021,0.063]). Interestingly, the AI system achieved a similar sensitivity as humans but at a higher specificity, emphasizing its potential use to discriminate normal cases as good as the best radiologists.

How does AI impact radiologists' performance in 2D mammography and DBT

In 2018, a study published in *Radiology* [9] showed that Transpara™ is the first AI-based software designed to assist radiologists reading mammograms that makes them more accurate without slowing them down.

In this fully-crossed multi-center retrospective reader study, a sample of 240 screening mammograms (of which 100 where screen-detected cancer, and 40 false positive recalls) were interpreted by 14 radiologists in the USA, once with and once without Transpara™ AI (version 1.3.0) in two distinct sessions. For each mammogram, the radiologists provided a forced Breast Imaging Reporting and Data System (BI-RADS) score and a level of suspicion (1–100, 100 meaning high suspicion of cancer). When reading with AI support, radiologists could benefit of all the features of the device as indicated above. The mammograms were from two different vendors (Siemens Healthineers MAMMOMAT Inspiration and Hologic Selenia Dimensions), and radiologists had on average 10 years of experience with breast cancer screening.

The impact of concurrent use of AI in radiologists' performance was analyzed in terms of accuracy (measured via AUC of the radiologists), specificity, sensitivity, and average reading time per mammogram.

On average, the radiologists' AUC was higher with AI support than with unaided reading (0.89 vs. 0.87, respectively; statistically significant, P = 0.002). For some radiologists, the improvement was up to 5% in terms of AUC. As seen in Figure 3, the increased performance was observed in the middle part of the ROC curve, suggesting that the AI system improves the evaluation of equivocal cases, where a second opinion is needed the most. In terms of recalls using the BI-RADS scoring, sensitivity increased with AI support (86% vs. 83% P = 0.046), whereas specificity trended toward improvement (79% vs. 77%, P = 0.06). The improvement in AUC was observed independently in all sub-analysis by lesion type, breast density, and mammography vendor. Another very important finding was that all radiologists trended to improve their accuracy with AI support, regardless of their experience, reducing the inter-reader variability (Fig. 4).

For the second endpoint of the study, reading time per screening mammogram, remained similar when using AI (3 seconds difference, 2%, P = 0.15). This was not the case when using traditional CAD systems, where reading time was higher [11].

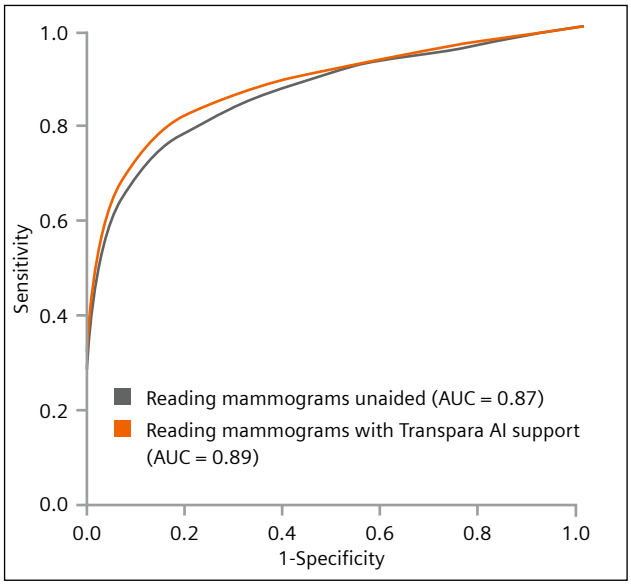

3 Average receiver operating characteristic curves of the 14 radiologists reading 2D mammograms unaided, and with support from Transpara™ AI. The area under the curve (AUC) is reported within parentheses.
Adapted from the publication in Radiology [9].

Recently, a new observer study with Transpara™ (to be presented at the European Congress of Radiology 2020) shows that radiologists also improve their cancer detection in DBT exams when using AI for support while simultaneously reading time is reduced.

The DBT study was performed by 9 radiologists (4–23 years of experience) who read DBT exams with synthetized 2D mammograms (Insight 2D) acquired with a Siemens Healthineers MAMMOMAT Inspiration device. Radiologists improved their accuracy performance in DBT when concurrently using AI (AUC + 0.041, P= 0.001, from 0.820 to 0.861), while reading time was on average -20% lower when using the system, down to approximately 30 seconds per DBT volume. Finally, the stand-alone performance of the AI system in DBT images was also found to be comparable to that of an average radiologist (95% CI of the difference = -0.038, 0.078). These findings are in line with the results in DM for the same system and with other results in literature for DBT [12].

How can AI optimize the efficiency of screening programs?

Early studies indicate that AI can improve radiologists' performance reading mammograms. In a screening setting, the concurrent use of AI has therefore the potential to positively impact in terms of more homogeneous reading performance across sites, reduction in false negative and false positive assessments.

But beyond its concurrent use, given the radiologist-comparable stand-alone accuracy detecting breast cancer in mammograms, AI could potentially be used as an effective independent reader of the screening process, or as a triaging tool for screening mammograms [13].

Given that more than 95% of screening exams do not contain any abnormality, it could be hypothesized that AI can filter out a large proportion of these normal exams automatically. Preliminary studies indicate that current AI could confidently label up to 50% of screening mammograms, with little error (2%–7%) [13, 14] (see Figure 5 for an example). In screening settings where double reading of screening mammograms is performed, this 50% of screening mammograms could, for example, undergo single reading instead of double reading. Having one reader in the loop for these exams could ensure that the cancers in the group are not automatically missed, and also potentially reduce the false positive recalls of the program: overall improving the positive predictive value. This is suggested by study published in *European Radiology* in 2019 [13], where it was observed that the decrease in sensitivity when not reading those mammograms with lowest AI scores is amply compensated by the increase in specificity, because less false positive assessments would be done (AUC reading only cases with scores 6–10 was non-inferior with non-inferiority margin 0.05 to the AUC reading all cases).

Triaging screening exams with AI could allow readers in some settings to focus on the cases with higher cancer prevalence (see Figure 2) when they are more attentive,

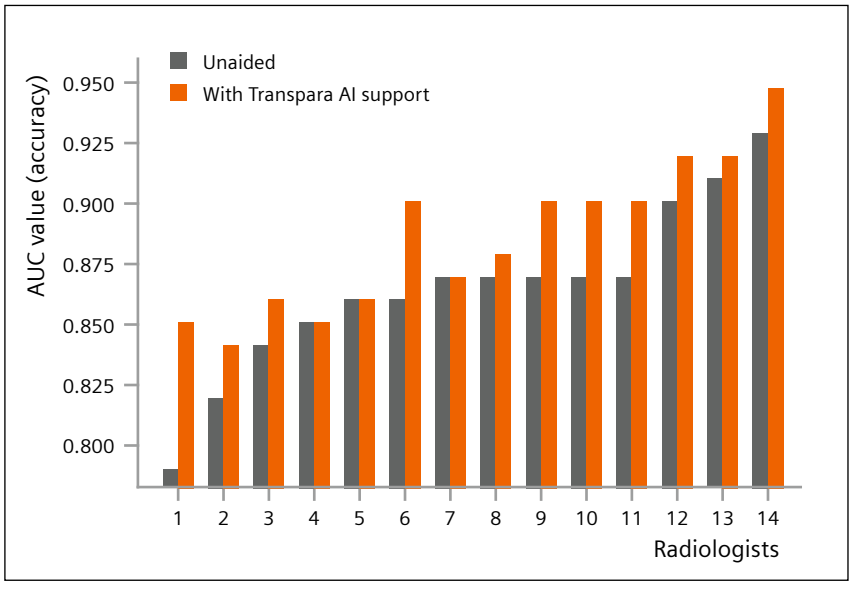

4 Area under the receiver operating characteristic curve (AUC) of each individual radiologists, reading 2D mammograms unaided and with Transpara™ AI support [9].

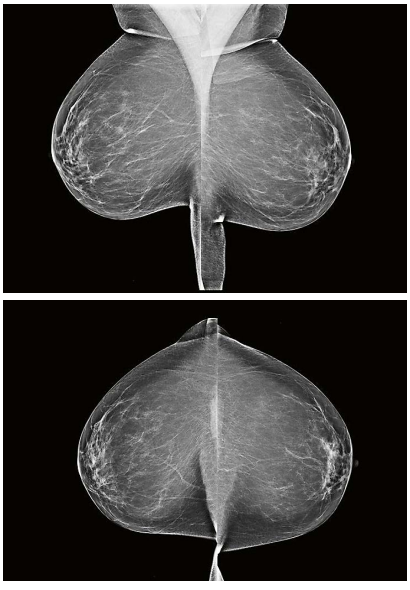

5 Example of a highly likely normal screening mammogram, labelled as Transpara™ AI with an exam score of 1, which was confirmed normal with two years follow-up round.

potentially also reducing the time that takes to recall women for diagnostic work-up. When considering the introduction of DBT for screening, using AI becomes more important to reduce workload given the increased reading time with DBT with respect to DM (up to twice as long) [15, 16].

Conclusion

Scientific studies are beginning to show convincing evidence that new generation breast AI systems can reach human-like performance and enhance the ability of radiologists to accurately detect breast cancer. In contrast to traditional CAD, these systems can be concurrently used and hold a great potential to reduce screening workload by acting as second reader, or by automatically labelling a large number of normal examinations with high negative predictive value. It is expected that with the continuous development in the field of AI some systems will soon begin to outperform most radiologists in a routine task such as mammography screening. This will enable more cost-effective screening scenarios in which the role of the human reader will change significantly. Before implementation, new screening methods involving AI should be validated thoroughly, while QA procedures for AI products have to be implemented to ensure safety and reliability of breast screening.

References

1 Lehman CD, Wellman RD, Buist DS, Kerlikowske K, Tosteson AN, Miglioretti DL, et al. Diagnostic Accuracy of Digital Screening Mammography With and Without Computer-Aided Detection. JAMA Unrestricted Med. 2015;175(11):1828-37.

2 Nishikawa RM, Bae KT. Importance of Better Human-Computer Interaction in the Era of Deep Learning: Mammography Computer-Aided Diagnosis as a Use Case. Journal of the American College of Radiology. 2018;15(1):49-52.

3 Litjens G, Kooi T, Bejnordi BE, Setio AAA, Ciompi F, Ghafoorian M, et al. A survey on deep learning in medical image analysis. Medical Image Analysis. 2017;42:60-88.

4 Bahl M. Detecting Breast Cancers with Mammography: Will AI Succeed Where Traditional CAD Failed? : Radiological Society of North America; 2018.

5 Trister AD, Buist DS, Lee CI. Will machine learning tip the balance in breast cancer screening? JAMA oncology. 2017;3(11):1463-4.

6 Kooi T, Litjens G, van Ginneken B, Gubern-Merida A, Sanchez CI, Mann R, et al. Large scale deep learning for computer aided detection of mammographic lesions. Med Image Anal. 2017;35:303-12.

7 Becker AS, Marcon M, Ghafoor S, Wurnig MC, Frauenfelder T, Boss A. Deep learning in mammography: diagnostic accuracy of a multipurpose image analysis software in the detection of breast cancer. Investigative radiology. 2017;52(7):434-40.

8 Mordang J-J, Janssen T, Bria A, Kooi T, Gubern-Mérida A, Karssemeijer N, editors. Automatic microcalcification detection in multi-vendor mammography using convolutional neural networks. International Workshop on Digital Mammography; 2016: Springer, Cham.

9 Rodríguez-Ruiz A, Krupinski E, Mordang J-J, Schilling K, Heywang-Köbrunner SH, Sechopoulos I, et al. Detection of Breast Cancer with Mammography: Effect of an Artificial Intelligence Support System. Radiology. 2018:181371.

10 Rodriguez-Ruiz A, Lång K, Gubern-Merida A, Broeders M, Gennaro G, Clauser P, et al. Stand-Alone Artificial Intelligence for Breast Cancer Detection in Mammography: Comparison With 101 Radiologists. JNCI. 2019;111(9).

11 Astley S, Gilbert FJ. Computer-aided detection in mammography. Clinical radiology. 2004;59(5):390-9.

12 Conant EF, Toledano AY, Periaswamy S, Fotin SV, Go J, Boatsman JE, et al. Improving Accuracy and Efficiency with Concurrent Use of Artificial Intelligence for Digital Breast Tomosynthesis. Radiology: Artificial Intelligence. 2019;1(4):e180096.

13 Rodriguez-Ruiz A, Lång K, Gubern-Merida A, Teuwen J, Broeders M, Gennaro G, et al. Can we reduce the workload of mammographic screening by automatic identification of normal exams with artificial intelligence? A feasibility study. European Radiology. 2019;29(9):4825-4832.

14 Yala A, Schuster T, Miles R, Barzilay R, Lehman C. A deep learning model to triage screening mammograms: a simulation study. Radiology. 2019:182908.

15 Zackrisson S, Lång K, Rosso A, Johnson K, Dustler M, Förnvik D, et al. One-view breast tomosynthesis versus two-view mammography in the Malmö Breast Tomosynthesis Screening Trial (MBTST): a prospective, population-based, diagnostic accuracy study. The Lancet Oncology. 2018;19(11):1493-503.

16 Rodriguez-Ruiz A, Gubern-Merida A, Imhof-Tas M, Lardenoije S, Wanders AJT, Andersson I, et al. One-view digital breast tomosynthesis as a stand-alone modality for breast cancer detection: do we need more? European Radiology. 2017;28(5):1938-1948.

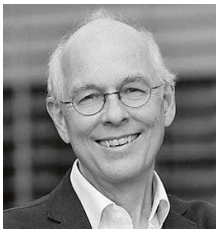

Professor
Nico Karssemeijer

Alejandro
Rodríguez-Ruiz

Contact

Alejandro Rodríguez-Ruiz, PhD
ScreenPoint Medical BV
Toernooiveld 300
6525 EC Nijmegen
The Netherlands
Tel. +31 24 202 0020
alejandro.rodriguezruiz@screenpointmed.com

Titanium Contrast-Enhanced Mammography (TiCEM): Mammography Becomes a Functional Technique

Arlette Elizalde, MD and Luis J. Pina Insausti, MD, PhD

Clínica Universidad de Navarra, Pamplona, Spain

Abstract

Digital Mammography has evolved into more accurate techniques, such as Digital Breast Tomosynthesis and Contrast Enhanced Dual Energy Mammography (CEDEM). CEDEM combines the high spatial resolution of Digital Mammography and the added value of neoangiogenesis. To obtain this functional information, the administration of intravenous iodinated contrast medium is required. A dual energy acquisition is performed: First, a low-energy image (similar to conventional DM) and immediately, during the same compression, a high-energy image is acquired (to detect the contrast uptake). MAMMOMAT Revelation has been developed to perform CEDEM. This system uses a titanium filter instead of a copper filter to reduce the tube load during the high-energy acquisition. For this reason, the contrast enhanced mammography technique is known as TiCEM (Titanium Contrast Enhanced Mammography). In our experience, TiCEM is more accurate than DM and offers morpho-functional information of breast lesions [1].

Introduction

Mammography-based breast screening is the only breast imaging technique that has been proven to reduce breast cancer mortality [2]. DM offers the highest spatial resolution of all the imaging modalities in a radiology department, being capable of detecting very subtle microcalcifications that can be the first sign of breast cancer. DM is usually the initial examination used in breast imaging and for breast cancer screening because it is a widely available and inexpensive technique. However, DM has a variable sensitivity that ranges from 50% to 85% and is especially low in dense breasts. It is well-known that the sensitivity of DM drops in dense breasts because of the overlapping tissue [3]. This low sensitivity has resulted in the introduction of complementary techniques such as ultrasound and digital breast tomosynthesis (DBT). DBT can significantly increase the sensitivity of DM from 60.4% to 81.1% [4].

Magnetic Resonance Imaging (MRI) of the breast is considered to be the most sensitive technique to detect breast cancer, especially invasive tumors. This high sensitivity is due to the use of intravenous contrast agents (gadolinium-based contrast media). Most breast cancers enhance at 1–2 minutes after the administration of i.v. contrast because of neoangiogenesis, i.e., new vessels with increased permeability. This is the reason why MRI is a morpho-functional technique. However, MRI of the breast is still an expensive technique, with little availability in many centres. Furthermore, it can have high false positive rates because many benign conditions can take up i.v. contrast. Finally, MRI is not always feasible in claustrophobic patients and in a small number of patients with certain metallic devices such as some metal implants, aneurysm clips, or pacemakers.

Contrast-enhanced dual energy Mammography

DM is a purely morphological technique, based on the attenuation of X-ray photons in the tumoral tissue. However, DM can become a morpho-functional technique

1 The MAMMOMAT Revelation performs Digital Mammography (DM), Digital Breast Tomosynthesis (DBT) and Contrast-Enhanced Dual Energy Mammography (CEDEM).

by using intravenous iodine-based contrast agents. The physiological mechanism for the detection of breast cancer is similar to MRI: the malignant lesions are detected due to neoangiogenesis. However, the contrast uptake of tumors cannot be shown on conventional DM because this technique uses low energy (23–28 kV). A specific energy level is required to detect the contrast agent, which is higher than conventional DM, ranging from 45 to 49 kV. That is why contrast-enhanced mammography uses dual energy: First, a low-energy image is acquired, similar to conventional DM, and immediately after, a high-energy image is also acquired to detect the contrast uptake. Both acquisitions are performed during the same compression. The high-energy image itself does not have diagnostic capabilities due to the high kV, which produces low tissue contrast and has a grey-appearance. For this reason, the system is optimized to create a recombined image by subtracting the low-energy image from the high-energy image.

This morpho-functional technique, known as Contrast-Enhanced Dual Energy Mammography (CEDEM), combines the high spatial resolution of DM with the information on neoangiogenesis. Both images, the low-energy (LE) and the recombined (R) ones, can be easily compared. This is a great advantage, because for one and the same lesion, the morphological and functional information is available at the same time [5].

The MAMMOMAT Revelation (Siemens Healthcare, Forchheim, Germany) uses a titanium filter instead of a copper filter for the high energy acquisition (Fig. 1). The commercial name for the CEDEM technique is TiCEM (Titanium Contrast-Enhanced Mammography). Its major advantage over other CEDEM techniques is better transmission with the same beam hardening, resulting in a reduced X-ray tube load. This allows for seamless examinations as the tube does not heat up as much while maintaining image quality [6].

Indications, contraindications, and risks

TiCEM is not intended to be used for the screening of a low risk population. The reasons are very simple: TiCEM uses i.v. contrast and a vein puncture is needed. Furthermore, the costs of the technique, although clearly lower than MRI, are higher than for DM.

The main indications of TiCEM are:

- Problem-solving technique: In a diagnostic setting, TiCEM can be used to evaluate palpable masses, asymmetries, mammographically detected masses, architectural distortions or any other doubtful findings on DM, DBT, or US.
- Assessment of recently diagnosed breast cancers: TiCEM can help in the detection of multifocal, multicentric, or bilateral cancers.
- Evaluation of response after neoadjuvant chemotherapy.
- Screening of selected groups: Intermediate risk women are those who have a higher risk of developing breast cancer in the future than the normal population but still have a risk of less than 25% during their lifetime (high risk women). This intermediate risk group comprises patients with a positive family history of breast cancer, some risk histological lesions (the known b3 histopathological lesions such as lobular carcinoma in situ, atypical ductal hyperplasia ...), patients with personal history of breast cancer, and those with extremely dense breasts.

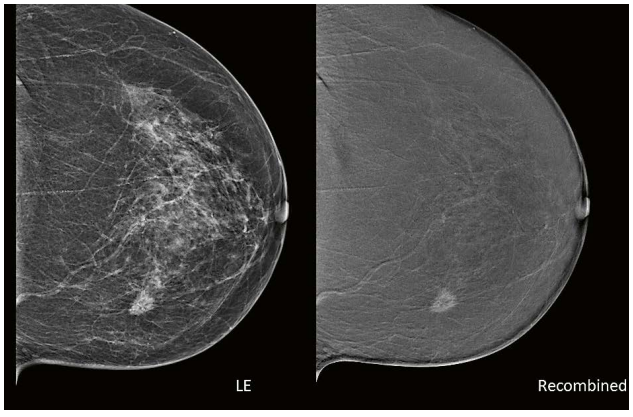

2 81-year-old lady who came to our institution because of a palpable lump in the left breast. The low-energy acquisition shows an irregular spiculated mass. The recombined image shows the enhancing mass and a subtraction of the normal fibroglandular tissue. Pathology: Invasive ductal carcinoma.

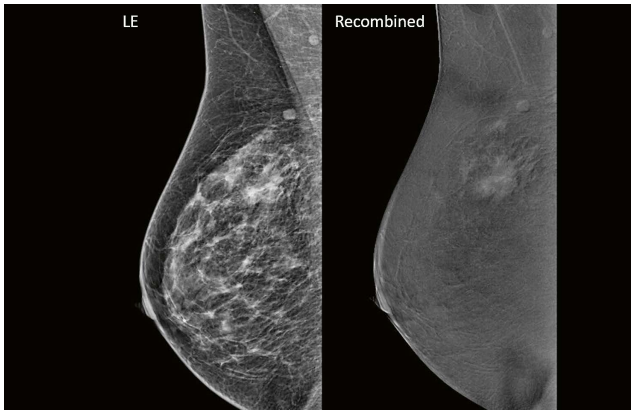

3 A 52-year-old woman attended at our institution with a palpable lump in the right breast. The low-energy image was considered normal. However the recombined image showed a suspicious enhancement, correlated with the palpable mass. Pathology: Invasive ductal carcinoma.

Contraindications
TiCEM is contraindicated for patients with a known allergy to iodinated contrast agents, pregnant patients, and those with renal insufficiency. Although it is not formally contraindicated, TiCEM is not intended for patients with breast implants or patients who are breast feeding.

Risks
The risks of TiCEM derive from the use of iodinated contrast agents. With the latest non-ionic iodinated contrast media, the incidence of hypersensitivity reactions is 0.7–3% [7]. Severe hypersensitivity reactions occur in only 0.02–0.04% of cases [8].

Description of the procedure

TiCEM is routinely performed in the mammography examination room. After a brief anamnesis to rule out allergy to iodinated contrast media, renal insufficiency, or pregnancy, informed consent is obtained. Then, an i.v. catheter is placed in a peripheral vein. An automatic injector is used for the administration of 1.5 mL per kg of iodinated contrast media at a rate of 3 mL per second. A delay is necessary for the perfusion of the contrast after the i.v. bolus (usually two minutes). Then the breast is compressed to obtain the images, usually starting with the pathological side. Several options can be offered: A unilateral study of the problematic breast (craniocaudal and MLO views) or a bilateral study using both views. During the same compression, the system acquires both the low-energy and high-energy images, which are quickly reconstructed and sent to a workstation for interpretation.

Our experience

We started implementing TiCEM examinations in October 2017. This technique was used as a problem solving technique and as an imaging modality to characterize breast lesions previously detected on DM, DBT, or US. Recently, we retrospectively assessed the TiCEM examinations that were performed at our institution. From October 2017 to June 2018, 80 patients with 120 histologically confirmed lesions were recruited.

Contact

Luis J. Pina Insausti, MD, PhD
Associate Professor
Department of Breast Imaging
Clínica Universidad de Navarra
36, Pío XII st
31008 Pamplona, Navarra
Spain
ljpina@unav.es

Three readers with different experience level in breast imaging (expertise, intermediate level, resident), blinded to the final diagnoses, evaluated both the low-energy (LE) and the recombined (R) images. The readers classified the lesions according to the BI-RADS categories.

Of the 120 lesions, 41 were benign and 79 malignant. The results were interpreted by means of ROC curves. The Area Under the Curve (AUC) of the combination LE+R was significantly larger than the AUC of LE alone for all the readers ($p<0.001$), irrespective of the experience of the reader (reader 1: 0.72 vs 0.86; $p< 0.001$; reader 2: 0.63 vs 0.80; $p<0.001$; reader 3: 0.70 vs 0.79; $p<0.001$). These data were similar for dense and non-dense breasts.

Conclusion

TiCEM is a new imaging modality that adds functional information to conventional mammography. This technique shares many of the indications of MRI, with the advantages of lower cost and better availability. In our experience, TiCEM shows better diagnostic accuracy than digital mammography, irrespective of the experience level of the radiologist.

References

1 González-Huebra I, Malmierca P, Elizalde A, Etxano J, Vejborg I, Uhlenbrock D, et al. The accuracy of titanium contrast-enhanced mammography: a retrospective multicentric study. Acta Radiol. 2020 [ahead of print].
2 Tabár L, Vitak B, Chen TH, Ming-Fang A, Cohen, Tot T, et al. Swedish two-county trial: impact of mammographic screening on breast cancer mortality during 3 decades. Radiology 2011;260: 658–663.
3 Pisano ED, Hendrick RE, Yaffe MJ, Baum JK, Acharyya S, Cormack JB, et al. Diagnostic accuracy of digital versus film mammography: exploratory analysis of selected population subgroups in DMIST. Radiology 2012;246:376–383.
4 Zackrisson S, Lång K, Rosso A, Johnson K, Dustler M, Förnvik D, et al. One-view breast tomosynthesis versus two-view mammography in the Malmö Breast Tomosynthesis Screening Trial (MBTST): a prospective, population-based, diagnostic accuracy study. Lancet Oncol. 2018 Nov;19(11):1493-1503.
5 Patel BK, Lobbes MBI, Lewin J. Contrast Enhanced Spectral Mammography: A Review. Semin Ultrasound CT MR 2018;39:70-79.
6 Knogler T, Homolka P, Hornig M, Leithner R, Langs G, Waitzbauer M, et al. Contrast-enhanced dual energy mammography with a novel anode/filter combination and artifact reduction: a feasibility study. Eur Radiol 2016;26:1575–1581.
7 Li X, Liu H, Zhao L, Liu J, Cai L, Liu L, et al. Clinical observation of adverse drug reactions to non-ionic iodinated contrast media in population with underlying diseases and risk factors. Br J Radiol 2017;90:20160729.
8 Katayama H, Yamaguchi K, Kozuka T, Takashima T, Seez P, Matsuura K. Adverse reactions to ionic and nonionic contrast media. A report from the Japanese Committee on the Safety of Contrast Media. Radiology 1990;175:621-8.

Assessing Breast Cancer Phenotypes with MRI Biomarkers in Clinical Practice

Elizabeth Morris, M.D.

Chief, Breast Imaging Service, Larry Norton Chair & Professor of Radiology,
Memorial Sloan Kettering Cancer Center (MSKCC), New York, NY, USA

Introduction

Advances in our understanding of the human genome have transformed the way we understand and treat breast cancer. Today, oncologists and gynecologists are no longer saying "this is invasive ductal carcinoma," but they can classify each breast cancer as one of four molecular subtypes based on its genetic expression. In this context, breast MRI provides a highly valuable and non-invasive tool to differentiate between subtypes due to the differences in imaging phenotypes between subtypes. In addition, as the cancer subtype has a significant impact on the individual patient's response to the currently available treatment options, MRI biomarkers may be used to predict complete response to therapy including non-surgical options and improve patient outcomes.

Breast cancer subtypes

While every breast cancer is unique, breast cancer can be classified into one of four distinct subtypes: luminal A, luminal B, human epidermal growth factor receptor 2 (HER2) positive, and basal-like. Luminal cancers are the most prevalent breast cancer subtype, representing 70% (55% luminal A, and 15% luminal B) of all breast cancers. Non-luminal cancers are less common but still substantial, representing 30% (15% basal-like and 15% HER2) of all breast cancers (Fig. 1).

The breast cancer subtype that is present in an individual patient has a significant impact on the cancer's aggressiveness. HER2-positive cancers and triple negative cancers are more highly aggressive whereas luminal A cancers (which are the most frequently diagnosed breast cancer) have a relatively good prognosis. In addition to the subtype, it must also be noted that intracellular receptors that respond to estrogen (ER) and progesterone (PR) hormones as well as HER2 receptors have been shown to also impact cancer aggressiveness. All cells have HER2 receptors on them, but if they overexpress these receptors to a certain degree, then they are associated with a much more aggressive form of breast cancer with uncontrolled growth.

Luminal A

Luminal A cancers are low-grade cancers that are strongly ER positive and/or PR positive as well as HER2 negative. They show no amplification of HER2, the proto-oncogene for increased growth, or Ki-67, a biomarker for cellular proliferation.

Luminal A cancers have a five-year survival rate of over 80%, which is highest among the subtypes. Luminal A cancers respond favorably to hormone therapy with tamoxifen or aromatase inhibitors (AI). Nonetheless, they are associated with the risk of late mortality more than ten years after the original diagnosis. It is hypothesized that the cancer cells remain inactive for a long time, probably suppressed by the immune system, before late relapse takes place. Late relapse is not uncommon with this subtype and luminal A cancers are highly likely to metastasize to the bone.

On MRI, luminal A presents as a typical spiculated mass with significant desmoplastic response (Fig. 2).

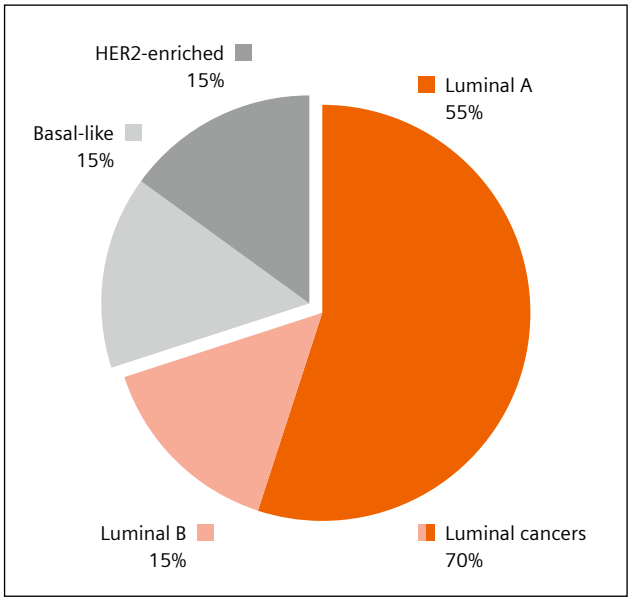

1 Breast cancer subtypes and their respective prevalence.

Luminal B

Luminal B cancers have a lower level of expression of ER and PR than luminal A cancers, and 20–30% of these cancers have a concomitant amplification of HER2. Compared with luminal A cancers, luminal B cancers are higher grade (always medium- to high-grade), showing a higher Ki-67 index and likely having lymph node involvement. Hence, luminal B cancers have a definite decrease in long-term survival, with a five-year survival of approximately 40%. Like luminal A cancers, luminal B cancers metastasize to the bone.

Mammoprint, Oncotype DX, and PAM-50 multigene assays identify breast cancers with an increased risk of recurrence based on gene expression arrays using formalin-fixed paraffin-embedded (FFPE) specimens. They help to identify which patient can forego chemotherapy. For luminal B cancers, a low Oncotype DX recurrence score permits the recommendation of hormonal therapy alone, whereas a high recurrence score indicates that chemotherapy is required as an adjunct treatment.

On imaging, luminal A and luminal B cancers look very similar. Tumor grading is the preferred mechanism for differentiating luminal A and luminal B cancers. Ki-67 can also provide great assistance but is not routinely recommended. Ki-67 as a prognostic marker is associated with larger tumor size, lymph node involvement, and shorter disease-free survival (DFS) and overall survival (OS). Ki-67 has shown to be positively associated with response to neoadjuvant chemotherapy (NAC).

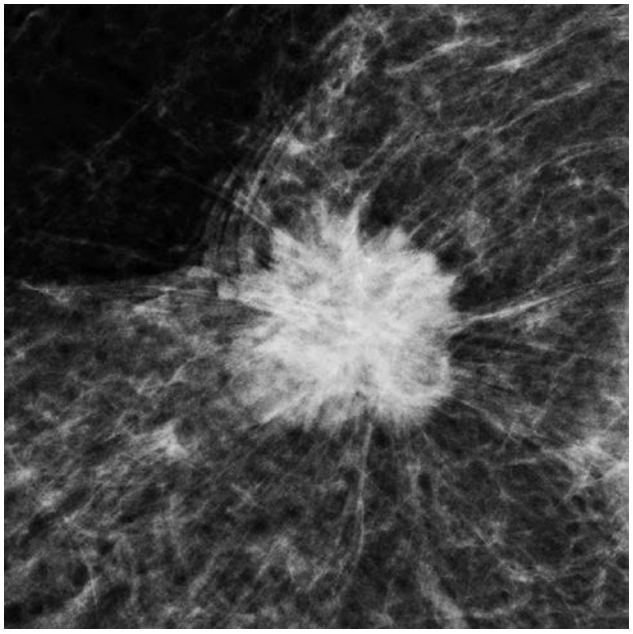

2 Zoomed T1-weighted post-contrast images (subtracted from T1-weighted pre-contrast) showing the typical representation of a luminal A breast cancer: a hyperdense, spiculated mass with irregular margins and significant desmoplastic response.

HER2 positive

15% of all breast cancers are HER2 positive. These tumors usually have an intermediate to high nuclear grade. Prior to the introduction of traztuzumab (brand name Herceptin) and pertuzamab (brand name Perjeta), the untreated clinical five-year survival rate was 31%; with these treatments, treating physicians have achieved a 33% reduction in mortality and a 52% reduction in recurrence.

Patients with HER2 positive cancers are more likely to have metastases that go to the viscera and the brain.

Basal-like

The fourth subtype of breast cancer is basal-like. Basal-like cancers have cells that are similar to epithelial cells (i.e., basal cells) that line the surface of the basement membranes along the ducts.

While there are many different types of basal cell cancer, the clinical focus is on triple-negative invasive ductal cancers. The discussion of triple-negative cancers generally centers on the very aggressive nature of this cancer and that it is more common in African-American women. In this population, this cancer represents 27% of the overall cancer burden and 41% of the cancer mortality.

Adenoid cystic carcinoma is a rare type of invasive ductal cancer; however, while it is triple negative, it has very positive prognosis and outcome.

Basal-like breast cancer is usually high grade with an aggressive clinical course. Recurrence normally occurs in the first five years after diagnosis. Once a patient is beyond the five-year mark, the prognosis is normally positive; this is in stark contrast to luminal A type breast cancer. Basal-like breast cancer also has a high occurrence of metastases to brain, lung, and viscera. This subtype of cancer has the highest mortality rate.

The role of MRI and radiomics

Over the past few decades, breast MRI capabilities have improved dramatically. With radiomics and radiogenomics, MR images can now be analyzed so that the image is related to the genome, rendering a host of data that might positively affect patient outcome. Radiologists can identify volumes to be segmented on MR images. Computers can then extract hundreds of descriptive and quantitative features that, when combined with medical and genomic data, create a comprehensive database. Clinicians can compare pixels with adjacent pixels and analyze them in this context to render many different datasets.

As opposed to traditional human interpretation where radiologists interpret the shape, margin, internal enhancement patterns, and kinetic curve of the lesion, computers can automatically segment abnormal lesions and parenchyma in the MR image, produce data on kinetic features, and analyze morphological texture features rendering a

more quantitative phenotype analysis. Radiomics has provided deeper analytic features in datasets, e.g., inter- and intra-tumor heterogeneity, site entropy, kurtosis, and site cluster dissimilarity, by extracting information from images that is imperceptible visually. This information is combined with clinical data and genomic profiles to facilitate the establishment of a clinically applicable prognosis prediction model. For example, MR images of a patient pre- and post-NAC as shown in in Figure 3 could render feature data that provide the clinician with a greater ability to predict pathologic complete response (pCR) by showing whether viable tumor persists.

While radiomics encompasses numerous potential features, these features tend to be standardizable and quantifiable. Many research organizations have been investigating the utility of radiomics to determine breast cancer phenotype groups. At Memorial Sloan Kettering Cancer Center (MSK), we have found that clinicians are able to predict breast cancer phenotypes with radiomics nearly as accurately as Oncotype DX and PAM50. Therefore, it is possible that in the future radiomics could establish oncologic signatures in the same way that tissue sampling currently does but without the need for invasive procedures.

Neoadjuvant Chemotherapy

Neoadjuvant Chemotherapy (NAC) is increasingly used to treat breast cancer because it enables breast-conserving surgery in women who traditionally require a mastectomy. The goal of NAC is pCR, defined as the absence of any residual in-situ or invasive cancer. pCR has served as a surrogate of DFS and OS for a long time.

Currently, the most accurately predictive test for pCR is MRI. MRI is more accurate in determining residual disease than physical examination, mammography, and ultrasound [3, 6]. However, MRI is not universally utilized as it still renders many false positives and false negatives. The absence of enhancement on MRI is called a radiologic complete response (rCR) even when there is a residual mass, and the pattern of the residual tumor is defined as contiguous or scattered to allow for better surgical selection.

With radiomics, it is possible that clinicians will achieve better response prediction with MRI, and MRI could potentially be used to replace surgery in the identification of patients with a complete response. Preliminary studies at MSK have shown that radiomics may be able to differentiate responders from non-responders.

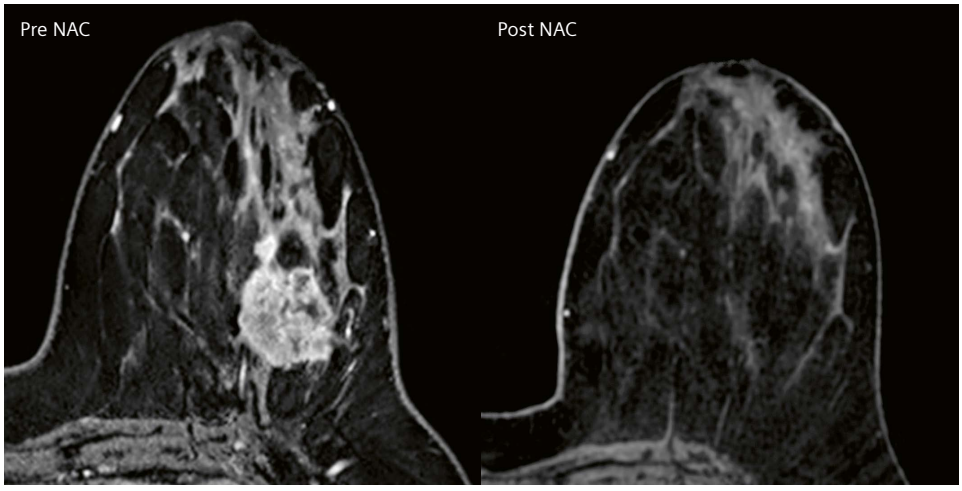

3 Subtracted, post-contrast T1-weighted images pre and post neoadjuvant chemotherapy. Patient showing complete imaging response which was confirmed as complete pathological response by biopsy. Highest response rates are seen in patients with TNBC and HER2+.

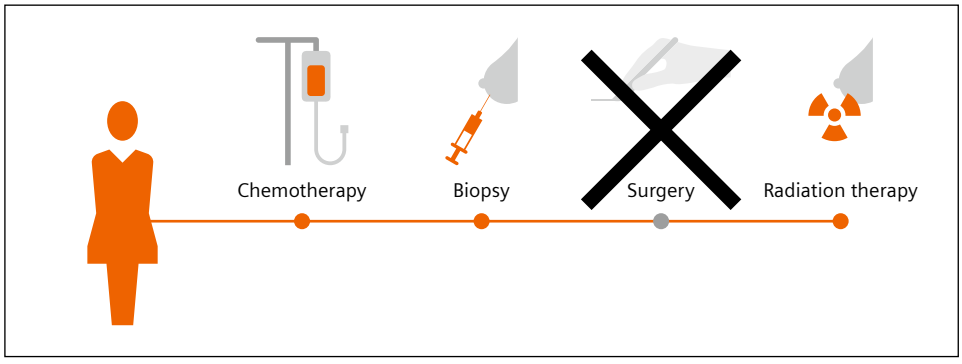

4 Proposed Care Pathway for patients with predicted pCR based on radiomic MRI profiling and biopsy-derived genetic profiling. In a planned trial patients shall proceed directly to radiation therapy without surgery.

New study conducted by Memorial Sloan Kettering Cancer Center

Currently, the NAC course of treatment involves MRI monitoring at critical points. We have been conducting a trial to perform a percutaneous MRI-guided biopsy in patients who have had an rCR as determined on MRI with radiomic analysis prior to surgery. We hypothesized that MRI-guided biopsy will accurately diagnose a pCR in women with complete response on MRI comparable to surgery, thus allowing us to avoid unnecessary surgery in these patients. For the pilot phase, so far ten patients have undergone the MRI-guided biopsy (with a marker to allow targeting of the biopsy) post NAC but prior to surgery. Results from the pilot phase indicate that MRI-guided biopsy can yield a high level of accuracy in diagnosing a pCR.

Therefore, we are currently proposing a full trial where the management of breast cancer in women with a pCR (as diagnosed by MRI-guided biopsy post-NAC) will proceed without surgery to the indicated duration of radiation therapy (Fig. 4). The salient open question is what quantity of residual disease precludes bypassing the surgical option for the less invasive method. Also, given that this would represent a new treatment protocol, the type of follow-up that would be required has yet to be determined.

Topics for further research

Another topic that is also worthy of further investigation is the association between parenchymal enhancement using contrast-enhanced MRI and the outcome of patients with breast cancer, as studied earlier by van der Velden et al. [4]. This study found that parenchymal enhancement is associated with long-term outcomes and higher parenchymal enhancement is associated with better outcomes. Women who have higher background enhancement who are treated experience better outcomes than women with lower background enhancement even though high background enhancement is associated with higher risk of developing breast cancer [4]. These results have been reproduced [5].

Contact

Elizabeth Morris
Chief, Breast Imaging Service,
Larry Norton Chair & Professor of Radiology
Memorial Sloan Kettering Cancer Center
1275 York Avenue
New York, NY, 10065
USA
Tel. +1 646 888 4510
morrise@mskcc.org

MRI features can also be investigated to predict cancer aggressiveness. For example, Lee et al. [1] found that spiculated margins were an indicator low grade ($p < 0.001$) and a low Ki-67 ($p = 0.007$); these are typical of luminal A breast cancers which have a high chance of pCR. Lee et al. also found that tumors with a high grade ($p < 0.001$) and that were ER negative were associated with poor patient outcome ($p = 0.001$).

Lastly, peritumoral edema, which indicates increased vascular permeability with local cytokines, is associated with early metastatic disease and can also be investigated for its clinical utility [2].

Conclusion

MR imaging is moving into an era of technology where the status quo is being disrupted. Artificial intelligence (AI) and machine learning will produce marked advancements in risk prediction and cancer detection.

As advances continue to be made in the tools available to clinicians, clinicians must ask themselves to find uses for these advancements that will improve treatment options, patient outcomes, and quality of life. Clinicians must be intellectually agile to use these tools to create new possibilities for the treatment of patients as individuals, guiding clinical practice toward personalized medicine.

References

1 Lee SH, Cho N, Kim SJ, Cha JH, Cho KS, Ko ES, Moon WK. Correlation between high resolution dynamic MR features and prognostic factors in breast cancer. Korean J Radiol. 2008 Jan-Feb;9(1):10-8.
2 Rao A, Net J, Brandt K, Huang E, Freymann J, Burnside E, Kirby J, Morris E, Bonaccio E, Giger M, Jaffe C, Ganott M, Sutton E, Le-Petross H, Zuley M, Dogan B, and Whitman G. TU-CD-BRB-07: Identification of Associations Between Radiologist-Annotated Imaging Features and Genomic Alterations in Breast Invasive Carcinoma, a TCGA Phenotype Research Group Study. Med Phys. 2015;42:3603-4.
3 Rosen EL, Blackwell KL, Baker JA, Soo MS, Bentley RC, Yu D, Samulski TV, Dewhirst MW. Accuracy of MRI in the detection of residual breast cancer after neoadjuvant chemotherapy. AJR Am J Roentgenol. 2003 Nov;181(5):1275-82.
4 van der Velden BH, Dmitriev I, Loo CE, Pijnappel RM, Gilhuijs KG. Association between Parenchymal Enhancement of the Contralateral Breast in Dynamic Contrast-enhanced MR Imaging and Outcome of Patients with Unilateral Invasive Breast Cancer. Radiology. 2015 Sep;276(3):675-85.
5 van der Velden BH, Sutton EJ, Carbonaro LA, Pijnappel RM, Morris EA. Contralateral parenchymal enhancement on dynamic contrast-enhanced MRI reproduces as a biomarker of survival in ER-positive/HER2-negative breast cancer patients. Euro Radiology. 2018 Nov;28(11):4705-16.
6 Yeh E, Slanetz P, Kopans DB, Rafferty E, Georgian-Smith D, Moy L, Halpern E, Moore R, Kuter I, Taghian A. Prospective comparison of mammography, sonography, and MRI in patients undergoing neoadjuvant chemotherapy for palpable breast cancer. AJR Am J Roentgenol. 2005 Mar;184(3):868-77.

Learn more!

Don’t miss the talks delivered by experienced and renowned experts at
www.siemens.com/magnetom-world > Clinical Corner > Clinical Talks
www.siemens-healthineers.com/mammography > Clinical Corner > Clinical Talks

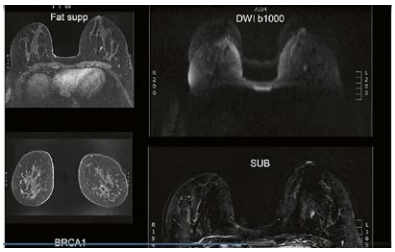

Phenotype-genotype correlation and radiological screening for breast cancer in gene mutation carriers
Chantal Van Ongeval
(UZ Leuven Campus Gasthuisber, Leuven, Belgium)

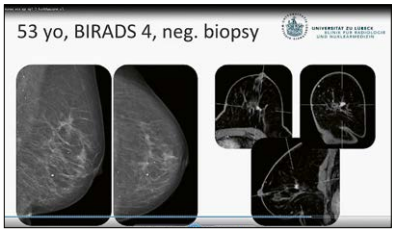

Gadolinium retention – impact on breast MRI?
Jörg Barkhausen
(University Hospital of Lübeck, Germany)

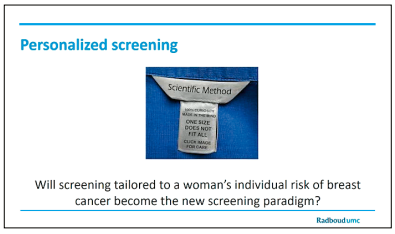

Personalized breast cancer screening and the role of breast density
Mireille Broeders
(Radboud University, Nijmegen, Netherlands)

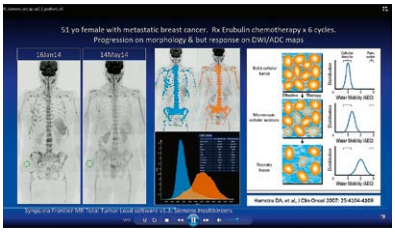

Progress on whole body MRI use for advanced breast cancer
Anwar Padhani
(Paul Strickland Scanner Centre, Mount Vernon Cancer Centre, Northwood, Middlesex, UK)

Final results of the Malmö Breast Tomosynthesis Screening Trial
Sophia Zackrisson
(Lund University, Malmö, Sweden)

ABVS and personalised breast cancer screening
André Grivegnée
(Institut Jules Bordet, Brussels, Belgium)

On account of certain regional limitations of sales rights and service availability, we cannot guarantee that all products included in this brochure are available through the Siemens sales organization worldwide. Availability and packaging may vary by country and is subject to change without prior notice. Some/All of the features and products described herein may not be available in the United States.

The information in this document contains general technical descriptions of specifications and options as well as standard and optional features which do not always have to be present in individual cases, and which may not be commercially available in all countries.

Due to regulatory reasons their future availability cannot be guaranteed. Please contact your local Siemens organization for further details.

Siemens reserves the right to modify the design, packaging, specifications, and options described herein without prior notice. Please contact your local Siemens sales representative for the most current information.

Note: Any technical data contained in this document may vary within defined tolerances. Original images always lose a certain amount of detail when reproduced.

This whitepaper is not for use in the USA.

Siemens Healthineers Headquarters
Siemens Healthcare GmbH
Henkestr. 127
91052 Erlangen, Germany
Phone: +49 9131 84-0
siemens-healthineers.com

Published by Siemens Healthcare GmbH · Order No. A91XP-300053E1-7600 · Printed in Germany · 8593 0520 ·